[redacted]

Copy
RM E50A19

[redacted]

copy 2

NACA RM E50A19

NACA

RESEARCH MEMORANDUM

ALTITUDE PERFORMANCE AND OPERATIONAL CHARACTERISTICS OF 29-INCH-DIAMETER TAIL-PIPE BURNER WITH SEVERAL FUEL SYSTEMS AND FUEL-COOLED STAGE-TYPE FLAME HOLDERS ON J35-A-5 TURBOJET ENGINE

By Richard L. Golladay and Harry E. Bloomer

Lewis Flight Propulsion Laboratory
Cleveland, Ohio

CLASSIFICATION CHANGED
UNCLASSIFIED

To ____________________ Effective Jan 20, 1958

By authority of NACA Res abs TRN-124

AMT 2-12-58

CLASSIFIED DOCUMENT

This document contains classified information affecting the National Defense of the United States within the meaning of the Espionage Act, USC 50:31 and 32. Its transmission or the revelation of its contents in any manner to an unauthorized person is prohibited by law. Information so classified may be imparted only to persons in the military and naval services of the United States, appropriate civilian officers and employees of the Federal Government who have a legitimate interest therein, and to United States citizens of known loyalty and discretion who of necessity must be informed thereof.

NATIONAL ADVISORY COMMITTEE FOR AERONAUTICS

WASHINGTON
April 28, 1950

[redacted]

NATIONAL ADVISORY COMMITTEE FOR AERONAUTICS

RESEARCH MEMORANDUM

ALTITUDE PERFORMANCE AND OPERATIONAL CHARACTERISTICS OF 29-INCH-DIAMETER TAIL-PIPE BURNER WITH SEVERAL FUEL SYSTEMS AND FUEL-COOLED STAGE-TYPE FLAME HOLDERS ON J35-A-5 TURBOJET ENGINE

By Richard L. Golladay and Harry E. Bloomer

SUMMARY

An investigation of thrust augmentation was conducted on an axial-flow-compressor turbojet engine in the NACA Lewis altitude wind tunnel over a range of simulated flight conditions. Performance and operational characteristics of several fuel-cooled stage-type flame holders and fuel systems were determined for a 29-inch-diameter tail-pipe burner.

Operation with a three-stage-type flame holder having the large stage upstream was the most efficient. Injecting fuel upstream of the flame holder increased the combustion efficiency slightly at high altitude, but the data were inconclusive at lower altitudes. Of the five stage-type flame holders investigated, the highest combustion efficiency was 0.87 and was obtained with the flame holder having three stages; however, the performance obtained in another investigation with a two-annular V-gutter flame holder was slightly better than with the stage-type flame holders.

INTRODUCTION

In a broad research program on thrust augmentation being conducted at the NACA Lewis laboratory, investigations (references 1 to 4) have shown that utilization of the tail-pipe-burning cycle is a practical means of increasing the thrust of turbojet engines. As part of this research program, an investigation of the effect of tail-pipe-burner design variables on burner performance and operation over a wide range of simulated-flight conditions is being conducted in the Lewis altitude wind tunnel. Part of this investigation is reported in references 5 and 6. In order

[redacted]

to obtain information that could be applied in designing tail-pipe burners, a study was made to determine the effect of flame-holder design, methods of fuel injection, and burner dimensions on the following burner requirements:

1. Maximum thrust with high combustion efficiency

2. Stable burner operation over a wide range of fuel-air ratios and flight conditions

3. Adequate tail-pipe cooling

4. Dependable starting

5. Minimum loss in thrust with burner inoperative

The work reported in references 1 to 4 was largely devoted to exploratory investigations, during which some of the general performance and operational characteristics of tail-pipe burners were determined. The results of these investigations established the background necessary to plan the present phase of afterburner research so as to cover the important considerations of tail-pipe-burner design.

In the phase of the tail-pipe-burning work reported herein, the effect of fuel distribution with several fuel-cooled stage-type flame holders on burner performance and range of stable combustion was studied in a 29-inch-diameter tail-pipe burner installed on a J35-A-5 turbojet engine. This study of stage-type flame holders represents an effort to achieve an increase in combustion efficiency by partly submerging the latter stages of the flame holders in the flame from the preceding stage. Because of the requirement that the successive stages of the flame holders be cooled, it was necessary to use fuel as the coolant. Fuel was therefore injected from the flame holder.

With each configuration, data were obtained over a range of simulated-flight conditions and tail-pipe-burner fuel-air ratios. These data are compared to show the effect of fuel distribution and flame-holder type on tail-pipe combustion efficiency and exhaust-gas temperature. The over-all performance of the two configurations that had the highest combustion efficiency are compared with the best configuration reported in reference 5. Altitude operating range, tail-pipe fuel ignition, and shell cooling are also discussed.

APPARATUS

Engine

The J35-A-5 engine used in this investigation has an 11-stage axial-flow compressor, eight cylindrical through-flow combustion 1245 chambers, and a single-stage turbine. The sea-level static thrust is 4000 pounds at an engine speed of 7700 rpm and a turbine-outlet temperature of 1250° F (1710° R). At this operating condition, the air flow is approximately 75 pounds per second and the fuel consumption is 4400 pounds per hour. The over-all length of the engine with standard-engine tail pipe is about 15 feet and the maximum diameter is about 38 inches. The rated operating condition of the standard engine was obtained with a $16\frac{15}{32}$-inch-diameter exhaust nozzle.

Fuel conforming to specification AN-F-32 (kerosene), with a lower heating value of 18,550 Btu per pound and a hydrogen-carbon ratio of 0.155, was used in the engine. Fuel conforming to specification AN-F-48b, grade 80, unleaded gasoline, with a lower heating value of 19,000 Btu per pound and a hydrogen-carbon ratio of 0.186, was used in the tail-pipe burner.

Installation

For this investigation, the standard-engine tail pipe was replaced by a tail-pipe-burner assembly attached to the turbine flange. The engine and tail-pipe burner were mounted on a wing section in the 20-foot-diameter test section of the altitude wind tunnel (fig. 1). Refrigerated air was supplied to the engine through a duct from the tunnel make-up air system. This duct was connected to the engine through a slip joint with a frictionless seal, which made possible the measurement of thrust with the tunnel-balance scale system. Air was throttled from approximately sea-level pressure to the desired pressure at the engine inlet; the pressure in the tunnel test section was maintained at the desired altitude. In order to simplify the installation and provide accessibility, no cowling was installed.

Tail-Pipe-Burner Assembly

The over-all length of the engine and tail-pipe burner was approximately $18\frac{1}{2}$ feet. The tail-pipe-burner assembly consisted of three sections: (1) a diffuser with an annular cross section, (2) a cylindrical burner section, and (3) a conical exhaust nozzle. A section drawing of the installation with a typical flame holder and fuel system installed is shown in figure 2. The outlet-to-inlet area ratio of the diffuser was 1.75. The burner section was 4 feet in length and had an inside diameter of 29 inches. A variable-area exhaust nozzle that would operate satisfactorily with tail-pipe burning was unavailable at the time of the investigation; a conical exhaust nozzle was therefore used.

1245

The flame holders used in this phase of the investigation were designed to provide annular flame seats at several stations in the burner section. The diameter of the annular flame seats either increased or decreased in uniform steps so that each stage of the flame holder after the first was located where it would be partly engulfed by the wake, and consequently by the flame, from the preceding stage. This flame-holder arrangement was investigated in an effort to improve the combustion efficiency by placing most of the flame-seating area in the vicinity of high-temperature burning gases, as indicated in reference 7. The main structural member of each stage was an Inconel tube through which fuel was circulated to prevent the stages engulfed in flame from overheating. These tubes also served as fuel injectors. Strips of 1/8-inch Inconel were welded to the tubes so as to form annular V gutters (fig. 3).

The five configurations of the fuel-cooled stage-type flame holder and fuel system investigated are shown in figure 4. The arrangements investigated in each configuration are indicated in the following table:

1245

Configuration	Figure	Flame holder	Projected area of flame holder (percent of total area)	Fuel-injection system
A	4(a)	Five-stage V-gutter contour; small stage upstream	56	Impinging jets directed upstream and downstream
B	4(b)	Five-stage V-gutter contour; large stage upstream	56	Impinging jets directed upstream and downstream. Also 12 impinging-jet fuel-injector bars located upstream of flame holder and spraying fuel upstream. Injectors used only for starting
C	4(c)	Two-stage V-gutter contour; large stage upstream	42	Jets directed upstream in large stage; orifices upstream and 45° inward on small stage
D	4(d)	Three-stage V-gutter contour; large stage upstream	59	Jets directed upstream
E	4(e)	Three-stage V-gutter contour; large stage upstream	59	Jets directed upstream of two rear stages only. Also 12 fuel-injector bars upstream of flame holder, spraying at right angles to gas flow

Configuration A. - The flame holder used in configuration A had five annular V-gutter stages and was arranged with the smallest-diameter stage upstream (fig. 4(a)). Impinging fuel jets were drilled in the upstream and downstream sides of each stage except for stage 1 (the small stage), which had jets on the upstream side only. These sets of impinging jets were equally spaced and arranged in such a manner that at each stage, except the first one, twice as much fuel was injected upstream as downstream. The orifices were located to provide a locally rich mixture over the first stage

and a uniform mixture over the remaining stages. Fuel was brought to the flame holder through three tubes located in the plane of the second stage and delivered to the other stages through three headers (fig. 3). No cooling liner was installed; an exhaust nozzle with an area of 321 square inches was used. At the downstream end of the diffuser inner cone a sheltered cone pilot for igniting the tail-pipe fuel was provided (figs. 5 and 6). The 1245
cone pilot was $8\frac{1}{4}$ inches in diameter and 4 inches deep; it was fitted with a conical fuel-spray nozzle and two spark plugs.

Configuration B. - The same annular V gutters were used in configuration B as in configuration A; however, the stages were arranged with the largest-diameter stage upstream (fig. 4(b)). Reversing the stages in configuration B was intended to induce more of the gases to flow toward the center of the burner where the velocity was initially low, thereby giving a more uniform velocity distribution across the burner than was obtained with configuration A. The impinging jets in the fuel tubes of each stage were the same as for configuration A; in addition, 12 impinging-jet fuel injectors were installed in the diffuser to aid in igniting the burner. A cooling liner was installed that extended from a plane 11 inches downstream of the burner-section inlet to the burner outlet. A 7/16-inch radial space was provided between the liner and the burner shell, through which flowed part of the gas at approximately turbine-outlet temperature. The exhaust-nozzle area was 316 square inches; the ignition system was the same as that used with configuration A.

Configuration C. - In order to determine the performance with a minimum number of flame-holding stages, configuration C (fig. 4(c)), which had only two stages, was investigated. The larger stage was located upstream. Fuel was injected in an upstream direction from both stages through orifices in the leading edges of the fuel tubes. In order to provide fuel at the center of the burner, part of the fuel in the second stage was injected through orifices toward the center of the burner at an angle of 45°. Fuel was independently supplied to each stage and it was possible to vary the fuel distribution between the stages during operation. For the performance data presented, approximately 50 percent of the fuel was injected through each stage. A cooling liner was installed that extended the full length of the burner section; a 1/2-inch radial space was provided between the liner and the burner shell. The exhaust-nozzle area and the ignition system were the same as those used with configuration B.

Configuration D. - The three stages of configuration D (fig. 4(d)) were designed to have about the same blocked area as configurations A and B; these stages were also located with the larger one upstream. Fuel was injected in an upstream direction from each stage through orifices in the leading edges of the fuel tubes. Fuel was provided to each of the stages independently and it was possible to vary the fuel distribution among the stages during operation. The performance data presented were obtained with approximately 65 percent of the fuel to the upstream stage, 20 percent to the middle stage, and 15 percent to the downstream stage. The cooling liner, the exhaust-nozzle area, and the ignition system were the same as those used with configuration C.

Configuration E. - The flame holder, the cooling liner, and the exhaust-nozzle area of configuration E (fig. 4(e)) were the same as those of configuration D. The fuel distribution, however, was changed from that of configuration D by injecting 25 percent of the fuel from the second and third stages of the flame holder and 75 percent from a set of 12 fuel injectors, which were located upstream of the flame holder. These injectors sprayed fuel at right angles to the gas flow. The tail-pipe fuel was ignited by a "torch igniter" (fig. 6), which consisted of a momentary injection of high-pressure fuel in one of the engine combustion chambers that resulted in a flash of flame through the turbine. This system is described in reference 5.

INSTRUMENTATION

Pressure and temperature instrumentation was installed at several measuring stations through the engine and tail-pipe burner (fig. 2). Engine air flow was measured by the use of survey rakes mounted at the engine inlet, station 1; a complete pressure and temperature survey was obtained at the turbine outlet, station 6; and static-pressure measurements were made at the burner-section inlet, station 7. A total-pressure survey was obtained 1 inch upstream of the exhaust-nozzle outlet, station 8, with a water-cooled survey rake. In order to obtain a correction that could be added to the scale thrust measurements, the drag of the water-cooled rake was obtained by means of a hydraulic-balance-piston mechanism. Engine and tail-pipe-burner fuel flows were measured by calibrated rotameters.

PROCEDURE

Operational characteristics were studied and performance data were obtained with the five tail-pipe-burner configurations over a range of simulated altitudes from 5000 to 40,000 feet and flight Mach numbers from 0.27 to 1.07. At each flight condition, the engine was operated at rated speed, 7700 rpm, and data were obtained over a range of tail-pipe fuel-air ratios. Dry refrigerated air was supplied to the engine at the standard temperature for each flight condition, except that the minimum temperature obtained was about -20° F. Total pressure at the engine inlet was regulated to correspond to the desired pressure at each flight condition with complete free-stream total-pressure recovery.

Because all the data were obtained with a fixed-area exhaust nozzle, limiting turbine-outlet temperature could be obtained with each configuration at only one value of tail-pipe fuel-air ratio at each flight condition. The burner performance obtained therefore does not represent the performance that might be obtained with a variable-area exhaust nozzle. The use of a fixed-area exhaust nozzle, however, provided the most expeditious means of comparing the performance of the various modifications. The over-all performance is presented as a function of flight Mach number for a turbine-outlet temperature of 1600° R. For configurations where the fuel distribution could be adjusted among the several planes of injection during operation, the fuel distribution was systematically varied until the maximum thrust was obtained at a given tail-pipe fuel-air ratio and flight condition. This distribution was then used to obtain burner performance over the operable range of flight conditions. Fuel distributions used for each of the configurations are indicated in table I.

The minimum tail-pipe fuel-air ratio was determined by lean combustion blow-out and the maximum fuel-air ratio by rich combustion blow-out, limiting turbine-outlet temperature, or the capacity of the fuel supply. Tail-pipe fuel-air ratio is defined as the ratio of the weight flow of tail-pipe fuel to the unburned air entering the tail pipe.

The values of thrust presented were measured with the balance scales and represent the actual thrust obtainable with the exhaust nozzle used. Exhaust-gas temperature was calculated from total-pressure measurements at the exhaust-nozzle outlet by an experimentally determined flow coefficient.

The probable limits of error in determining jet thrust, exhaust-gas temperature, and combustion efficiency are $\pm 1\frac{1}{2}$, ± 3, and ± 5 percent, respectively. The symbols and the methods of calculation used in the reduction of data are presented in the appendix.

RESULTS AND DISCUSSION

A preliminary investigation of stage-type flame holders in a $25\frac{3}{4}$-inch-diameter tail-pipe burner indicated that the fuel tubes alone would not serve as satisfactory flame holders. Strips of Inconel were therefore welded to the tubes so as to form annular V gutters, which would offer more restriction. This configuration offered some improvement, but was still unsatisfactory. The tail-pipe-burner diameter was then increased to 29 inches in order to decrease the velocities across the flame holder. The results of operation with this burner are presented graphically and represent typical performance of the configurations investigated. Data for the five configurations are presented in table I.

Comparison of Configurations

Arrangement of stages. - Results are presented for configurations A and B in figure 7 to show the effect of flame-holder-stage arrangement on the variation of combustion efficiency and exhaust-gas total temperature with tail-pipe fuel-air ratio. This comparison is made at altitudes of 5000 and 25,000 feet and a flight Mach number of 0.27. At an altitude of 5000 feet, the peak combustion efficiency was approximately 0.23 higher and the maximum exhaust-gas temperature was approximately 420° R higher with configuration B than with configuration A. At an altitude of 25,000 feet, the maximum combustion efficiency was only about 0.04 higher for configuration B, but the maximum efficiency occurred at a tail-pipe fuel-air ratio of about 0.0425 as compared to 0.022 with configuration A. As a result, the maximum exhaust-gas temperature obtained at an altitude of 25,000 feet was approximately 480° R higher with configuration B than with configuration A.

With the arrangement of configuration A, the flame holder constituted a restriction that diverted part of the flow toward the wall of the burner. As a result, the velocity profile that normally exists at the burner inlet with higher velocities near the shell than in the center of the burner was further accentuated.

The stages were reversed in configuration B so that the restriction offered by the flame holder would divert the gas toward the center of the burner and thereby give a more uniform velocity profile. The lower combustion efficiencies obtained with configuration A are attributed to the higher velocity over the large-diameter stages in addition to the mean fuel-injection station being located farther downstream. The burner-shell temperature was higher for configuration B than for A because of the higher gas temperature; however, the cooling liner provided adequate shell cooling.

Flame holders. - Results are presented for configurations B, C, and D in figures 8 and 9 to show the effect of the flame holder used on the variation of combustion efficiency and exhaust-gas total temperature, respectively, with tail-pipe fuel-air ratio. This comparison is made at altitudes of 5000, 25,000, and 35,000 feet and a flight Mach number of 0.27. Configurations B, C, and D had five, two, and three stages, respectively. The effect of the number of stages on the performance is not isolated in this comparison, inasmuch as the width of the annular V gutters was greater for configurations C and D than for configuration B. Scale effect is therefore included in the comparison and the blocking area does not vary in proportion to the number of stages.

At an altitude of 5000 feet, the performance of configurations B and D was about the same at tail-pipe fuel-air ratios above approximately 0.028. The peak combustion efficiency for configuration C was approximately 0.14 lower than for configurations B and D. At an altitude of 25,000 feet, the highest and lowest combustion efficiencies and exhaust-gas total temperatures were obtained with configurations D and B, respectively. At an altitude of 35,000 feet, the combustion efficiency and the exhaust-gas total temperature were approximately the same for configurations C and D and were lower for configuration B. The more rapid decrease in the over-all combustion efficiency and exhaust-gas total temperature of configuration B with an increase in altitude was probably due to scale effect, because the flame-holder gutters were narrower with this configuration than for the others. The fact that the combustion efficiency and exhaust-gas total temperature for configuration D were generally higher than for configuration C was probably due to the 17-percent greater flame-holder blocking area of configuration D. This effect was not as apparent at an altitude of 35,000 feet as at lower altitudes.

Fuel distribution. - Results are presented for configurations D and E in figure 10 to show the effect of injecting part of the fuel in the diffuser section upstream of the flame holder on the

variation of combustion efficiency and exhaust-gas total temperature with tail-pipe fuel-air ratio. This comparison is made for altitudes of 5000 and 35,000 feet and a flight Mach number of 0.27. With configuration D, all the fuel was injected from the three
1245 flame-holder stages; with configuration E, one-fourth of the fuel was injected from the two downstream stages of the three-stage flame holder and three-fourths of the fuel was injected through the fuel injectors upstream of the flame holder. At an altitude of 5000 feet, the maximum combustion efficiency obtained with configuration E was about 0.08 lower than the peak efficiency for configuration D. The data indicated, however, that peak combustion efficiency was not reached with configuration E, and that the peak efficiency would occur at tail-pipe fuel-air ratios in excess of 0.035 as compared to 0.028 with configuration D. The variation of exhaust-gas total temperature at this altitude substantiated this trend in that the data indicated that the temperature for configuration E would exceed that of configuration D at tail-pipe fuel-air ratios slightly higher than those investigated. At an altitude of 35,000 feet, the peak combustion efficiency was about 0.15 higher and the maximum exhaust-gas total temperature was about 180° R higher for configuration E. The very low combustion efficiencies and temperatures that occurred at low tail-pipe fuel-air ratios were presumably caused by combustion blow-out at some of the flame-holder stages. Data for an altitude of 5000 feet were inadequate to indicate any definite rise in combustion efficiency and exhaust-gas temperature from injecting most of the fuel upstream of the flame holder. Data for an altitude of 35,000 feet, however, show a definite increase in combustion efficiency as a result of injecting most of the fuel upstream of the flame holder and are therefore in agreement with similar results presented in reference 3. This improvement in performance is probably due to better radial distribution of fuel and the longer length for mixing and vaporization of the fuel.

Burner Performance

Data for configuration D were selected to show the variation of burner-inlet conditions with altitude and flight Mach number and to demonstrate the effect of tail-pipe-burner-inlet conditions on combustion efficiency and exhaust-gas temperature (figs. 11 to 13). These data were selected because the combustion efficiency with this configuration was higher over a wider range of altitudes and flight Mach numbers than for the others investigated, as shown in figures 8 and 10.

Effect of altitude and flight Mach number. - As the tail-pipe fuel-air ratio was increased at each altitude and flight Mach number, the turbine-outlet pressure and temperature increased and the burner-inlet velocity remained approximately constant (figs. 11 and 12). At a constant tail-pipe fuel-air ratio, the turbine-outlet pressure decreased approximately in proportion to the atmospheric pressure; the turbine-outlet temperature was reduced slightly 1245
as the altitude was increased from 5000 to 40,000 feet at a flight Mach number of 0.27 (fig. 11). Turbine-outlet pressure decreased approximately in proportion to the engine-inlet total pressure; the turbine-outlet temperature increased slightly as the flight Mach number was lowered from 0.92 to 0.27 at an altitude of 25,000 feet; the effect of flight condition on the burner-inlet velocity was negligible (fig. 12).

Increasing the altitude from 5000 to 40,000 feet decreased the peak combustion efficiency from 0.82 to 0.50 (fig. 13(a)). Because the effect of variations in altitude upon the burner-inlet velocity and turbine-outlet total temperature was slight (figs. 11(a) and (b)), this variation in efficiency was primarily due to the change in turbine-outlet pressure from approximately 3200 to 700 pounds per square foot (fig. 11(c)). With this decrease in turbine-outlet pressure, there was an attendant increase from approximately 0.028 to 0.042 in the tail-pipe fuel-air ratio at which peak combustion efficiency occurred. As the turbine-outlet pressure was decreased from about 3200 to 1700 pounds per square foot (fig. 11(c)), the peak combustion efficiency varied between 0.82 and 0.76 (fig. 13(a)). Combustion efficiencies did not vary uniformly with turbine-outlet pressure over this range of pressures; this effect is attributed to inaccuracies in the measurement of exhaust-gas pressures. A further decrease in pressure to about 1000 pounds per square foot decreased the peak combustion efficiency to approximately 0.56. These results indicate that with configuration D the combustion efficiency is much more adversely affected by reductions in turbine-outlet pressure below about 1700 pounds per square foot than at higher pressures.

A decrease in the flight Mach number from 0.92 to 0.27 at an altitude of 25,000 feet, which was accompanied by a reduction in turbine-outlet pressure from about 2500 to 1700 pounds per square foot (fig 12(c)), reduced the peak combustion efficiency from 0.87 to 0.76 (fig. 13(a)). This change in combustion efficiency with turbine-outlet pressure is more than that obtained for a greater pressure change accompanying a variation in altitude. The variation of combustion efficiency with flight Mach number was apparently magnified by discrepancies in exhaust-gas pressure measurements.

Exhaust-gas total temperature increased with fuel-air ratio at each condition investigated. The effect of decreases in turbine-outlet pressure as the altitude was increased at constant flight Mach number and as the flight Mach number was decreased at constant altitude on the exhaust-gas temperature was similar to the effect on the combustion efficiency (fig. 13(b)). In order to obtain a given exhaust-gas temperature, it was necessary to increase the tail-pipe fuel-air ratio as the turbine-outlet pressure was decreased; this condition was due to the reduction in combustion efficiency.

Over a range of turbine-outlet pressures from 3200 to 1700 pounds per square foot (corresponding to altitudes of 5000 to 25,000 feet), the exhaust-gas temperature ranged from approximately 2800° to 3110° R (fig. 13(b)). Higher exhaust-gas temperatures could have been obtained with higher tail-pipe fuel-air ratios.

Over-all Performance

Inasmuch as data were obtained over a range of flight Mach numbers for configurations B and D only, results are presented for these configurations to show the variation of over-all performance with flight Mach number at an altitude of 25,000 feet and a turbine-outlet temperature of 1600° R. Also presented for these same conditions are data obtained with the best configuration in reference 5. This configuration consisted of an uncooled two-annular-V-type flame holder installed in the 29-inch-diameter tail-pipe burner with 12 fuel-spray bars mounted upstream of the flame holder in the diffuser section. The variation of exhaust-gas total temperature and augmented thrust ratio with flight Mach number is shown in figure 14. Augmented thrust ratio is defined as the ratio of the net thrust obtained with tail-pipe burning to the net thrust obtained at the same turbine-outlet conditions with the standard tail pipe installed. With configuration D, the thrust ratio increased from 1.33 to 1.56 as the flight Mach number was increased from 0.27 to 0.92. This increase in thrust ratio was accompanied by a rise in the exhaust-gas total temperature from 2900° to 3070° R.

Variation of the tail-pipe-burner combustion efficiency with flight Mach number is shown in figure 15(a). Variation of specific fuel consumption based on net thrust with flight Mach number for the tail-pipe burner operating and also with the standard tail pipe installed is shown in figure 15(b). With configuration D, the tail-pipe-burner combustion efficiency increased from 0.75 to 0.87 as the flight Mach number was increased from 0.27 to 0.92.

This increase in combustion efficiency was accompanied by a decrease in specific fuel consumption based on net thrust from 2.46 to 2.42. The specific fuel consumption of the engine with the standard tail pipe increased from 1.2 to 1.35 over this same range of flight Mach numbers.

As shown in figures 14 and 15, the performance of the best stage-type flame holder (configuration D) was inferior to that of 1245
the best two-annular V-type flame holder of reference 5. Because the pressure losses for the two configurations were approximately the same, this difference was possibly due to the compromise made by injecting part of the fuel at the flame holder and thereby causing poor fuel distribution and a shorter time for burning.

Tail-Pipe Pressure Losses

Tail-pipe total-pressure-loss ratio with burning is presented in figure 16 as a function of exhaust-gas total temperature for each configuration. Tail-pipe pressure-loss ratio is defined as the ratio of the loss in total pressure between the turbine outlet and the exhaust-nozzle outlet to the total pressure at the turbine outlet. The pressure-loss ratio was approximately constant at 0.06 for exhaust-gas temperatures between 2300° and 3000° R for all configurations. The pressure-loss ratio with the standard engine tail pipe was approximately 0.01 (reference 5).

Operational Characteristics

The tail-pipe burner was operated at fuel-air ratios from approximately 0.011 to 0.068 and turbine-outlet temperatures from 1000° to 1690° R at numerous simulated-flight conditions. Complete performance data as shown in table I, however, were not obtained at all these conditions. During operation over this range of conditions, various operational characteristics observed included rich and lean blow-out, tail-pipe fuel ignition, tail-pipe-burner shell temperature, and steadiness of combustion. Knowledge of these characteristics is important in the design and the operation of tail-pipe burners. A few of the characteristics of each configuration are presented in the following discussion.

<u>Combustion characteristics</u>. - With configuration A, the tail-pipe burner was operated over a range of fuel-air ratios from 0.013 to 0.067 at an altitude of 25,000 feet; however, burning at 5000 feet was subject to pulsations with attendant fluctuations in pressure

and fuel flow, apparently caused by fuel vaporization in the fuel tubes. The flame filled the exhaust nozzle only at altitudes above 5000 feet. Visual observation indicated that the mixture in the center of the flame was rich; the tail pipe and the nozzle always remained cool during operation.

Configuration B, in which the flame holder used for configuration A was reversed, produced more even burning in the tail pipe and a full nozzle of flame. Some burning fluctuations occurred, however, at an altitude of 5000 feet. The nozzle was much hotter during high fuel-flow operation with configuration B than with A. The range of tail-pipe fuel-air ratios at 25,000 feet was 0.013 to 0.032 and limiting turbine-outlet temperature was reached.

When configuration C with a 50-50 fuel distribution to the two stages of the flame holder was used, the tail-pipe burner was operated over a range of fuel-air ratios from 0.013 to 0.051 at an altitude of 25,000 feet and 0.020 to 0.055 at 35,000 feet. Operation above 35,000 feet was unstable.

When configuration D was operated with 65 percent of the fuel flow to stage 1, 20 percent to stage 2, and 15 percent to stage 3, each stage was subject to flow fluctuations at several flight conditions. The tail-pipe fuel-air ratio range at an altitude of 25,000 feet was 0.020 to 0.037 and at 40,000 feet was 0.030 to 0.045. Operation above 40,000 feet was unstable.

With configuration E, runs were made with 75 percent of the fuel injected through 12 side-spray bars upstream of the flame holder and 25 percent through the two downstream stages of the flame holder. The tail-pipe fuel-air ratio ranged from 0.018 to 0.026 at 25,000 feet and from 0.022 to 0.031 at 35,000 feet. The tail-pipe burning was generally unsteady, because the flame did not appear seated on the entire flame holder except at limiting turbine-outlet temperatures above 1600° R.

Tail-pipe fuel ignition. - With the cone pilot (figs. 5 and 6), fuel ignition was effected at altitudes as high as 30,000 feet; the spark plug and the fuel nozzle in the pilot were, however, frequently burned away. Starts were usually made at engine speeds from 4000 to 6000 rpm. When the ignition system failed, the tail-pipe-burner fuel was ignited by rapidly accelerating the engine, which resulted in a burst of flame into the tail pipe. The torch igniter (fig. 6) was used only with configuration E. Several starts were effected up to an altitude of 27,000 feet at reduced engine speed. This method was later found to be very reliable for obtaining ignition at full engine speed at altitudes up to 50,000 feet, as discussed in reference 5.

Tail-pipe-burner-shell cooling. - Cooling of the tail-pipe-burner shell was effected by an inner liner in all configurations except A. Approximately 6 percent of the gas flow at turbine-outlet temperature passed between the liner and the shell. This flow provided sufficient cooling to keep the tail-pipe shell below a temperature of 1700° R. The liner temperatures were somewhat higher, but because the stresses on the liner were low, this condition was not critical. More extensive experimental results of cooling-liner investigations including methods of construction are presented in reference 5.

SUMMARY OF RESULTS

The following results were obtained from an investigation of a 29-inch-diameter tail-pipe burner with a fixed-area exhaust nozzle on a J35 turbojet engine in the NACA Lewis altitude wind tunnel:

1. The burner performance of the five-stage flame holder with the large stage upstream was markedly better than that with the large stage downstream.

2. The three-stage flame holder was more efficient than a five-stage flame holder with the large stage upstream, which had approximately the same blocking area, but narrower gutters. The three-stage flame holder was also more efficient than a two-stage flame holder with the same width gutters, but 17 percent less blocking area.

3. Injecting fuel upstream of the flame holder resulted in a reduction of combustion efficiency at an altitude of 5000 feet, but an increase at 35,000 feet.

4. The maximum combustion efficiency obtained was 0.87 with the three-stage flame holder with the large stage upstream. This value was obtained at an altitude of 25,000 feet, a flight Mach number of 0.92, and a tail-pipe fuel-air ratio of 0.037.

5. At an altitude of 25,000 feet and with a turbine-outlet temperature of 1600° R, the ratio of augmented to normal thrust increased from 1.33 at a flight Mach number of 0.27 to 1.56 at a

flight Mach number of 0.92 for the three-stage flame holder with the large stage upstream. This increase in thrust ratio was accompanied by a rise in exhaust-gas total temperature from 2900° to 3070° R, an increase in combustion efficiency from 0.75 to 0.87, and a decrease in specific fuel consumption from 2.46 to 2.42.

6. The performance of the stage-type flame holders investigated was inferior to that of the annular two-V flame holder subsequently investigated in the same burner.

7. One configuration was successfully operated at an altitude as high as 40,000 feet and most configurations were operated at altitudes as high as 35,000 feet at a flight Mach number of approximately 0.27.

Lewis Flight Propulsion Laboratory,
National Advisory Committee for Aeronautics,
Cleveland, Ohio.

APPENDIX - CALCULATIONS

Symbols

The following symbols are used in this report:

A	cross-sectional area, sq ft
B	thrust scale reading, lb
C_d	flow (discharge) coefficient, ratio of effective flow area to measured area
C_T	thermal-expansion ratio, ratio of hot-exhaust-nozzle area to cold-exhaust-nozzle area
C_v	exhaust-nozzle velocity coefficient, ratio of actual exhaust-nozzle velocity to ideal exhaust-nozzle velocity after expansion to free-stream static pressure
D	external drag of installation, lb
D_r	drag of exhaust-nozzle survey rake, lb
F_j	jet thrust, lb
F_n	net thrust, lb
f/a	fuel-air ratio
g	acceleration due to gravity, 32.2 ft/sec^2
H	total enthalpy, Btu/lb
h_c	lower heating value of fuel, Btu/lb
M	Mach number
P	total pressure, lb/sq ft absolute
P_8'	total pressure at exhaust-nozzle survey station in standard-engine tail pipe, lb/sq ft absolute
p	static pressure, lb/sq ft absolute
R	gas constant, ft-lb/(lb)($^{\circ}$R)

1245

T	total temperature, °R
T_i	indicated temperature, °R
t	static temperature, °R
V	velocity, ft/sec
W_a	air flow, lb/sec
W_c	bearing cooling-air flow, lb/sec
W_f	fuel flow, lb/hr
W_f/F_n	specific fuel consumption based on total fuel flow and net thrust, lb/(hr)(lb thrust)
W_g	gas flow, lb/sec
γ	ratio of specific heats for gases
η_b	combustion efficiency
ρ	static density, slugs/cu ft

Subscripts:

a	air
e	engine
f	fuel
g	gas
j	jet
m	fuel manifold
s	scale
t	tail-pipe burner
x	inlet duct at frictionless slip joint
0	free-stream condition

1 engine inlet

3 engine combustion-chamber inlet

6 turbine outlet (diffuser inlet)

7 static-pressure survey plane, $5\frac{3}{16}$ inches upstream of burner-section-inlet flange 1245

8 exhaust-nozzle total-pressure survey plane, 1 inch upstream of outlet

9 exhaust-nozzle outlet

Methods of Calculation

Flight Mach number and airspeed. - Flight Mach number and equivalent airspeed were calculated from the ram-pressure ratio by the following equations; complete pressure recovery at the engine inlet was assumed:

$$M_0 = \sqrt{\frac{2}{\gamma_1 - 1}\left[\left(\frac{P_1}{p_0}\right)^{\frac{\gamma_1 - 1}{\gamma_1}} - 1\right]} \tag{1}$$

$$V_0 = M_0 \sqrt{\gamma_1 g R T_1 \left(\frac{p_0}{P_1}\right)^{\frac{\gamma_1 - 1}{\gamma_1}}} \tag{2}$$

The equivalent free-stream total temperature was assumed equal to the compressor-inlet indicated temperature. The use of this assumption introduces an error in airspeed of less than 1 percent.

Air flow. - Air flow at the engine inlet was determined from pressure and temperature measurements obtained with four survey rakes in the inlet annulus. The following equation was used for calculation of air flow:

1245

$$W_{a,1} = p_1 A_1 \sqrt{\frac{2\gamma_1 g}{(\gamma_1 - 1)Rt_1}\left[\left(\frac{P_1}{p_1}\right)^{\frac{\gamma_1 - 1}{\gamma_1}} - 1\right]} \tag{3}$$

Bearing cooling air was bled from the compressor in a quantity approximately equal to the engine fuel flow. The air flow entering the engine combustion chamber was therefore calculated as follows:

$$W_{a,3} = W_{a,1} - W_c = W_{a,1} - \left(\frac{W_{f,e}}{3600}\right) \tag{4}$$

Temperatures. - Static temperatures were calculated from indicated temperatures by the adiabatic relation between temperature and pressure; the impact recovery factor was determined to be 0.85 for the type of thermocouple used:

$$t = \frac{T_i}{1 + 0.85\left[\left(\frac{P}{p}\right)^{\frac{\gamma - 1}{\gamma}} - 1\right]} \tag{5}$$

Tail-pipe gas flow. - The total weight flow through the tail-pipe burner was calculated as follows:

$$W_g = W_{a,3} + \frac{W_{f,e} + W_{f,t}}{3600} \tag{6}$$

Tail-pipe fuel-air ratio. - The tail-pipe fuel-air ratio used herein is defined as the weight flow of fuel injected into the tail-pipe burner divided by the weight flow of unburned air entering the tail-pipe burner from the engine. Weight flow of unburned air was determined by assuming that the fuel injected in the engine combustion chamber was completely burned. By combining air flow, engine fuel flow, and tail-pipe fuel flow, the following equation for tail-pipe fuel-air ratio was obtained:

$$(f/a)_t = \frac{W_{f,t}}{3600\ W_{a,3} - \frac{W_{f,e}}{0.067}} \tag{7}$$

where 0.067 is the stoichiometric fuel-air ratio for the engine fuel.

Turbine-outlet temperature. - Because the temperature measurements at station 6 were unreliable when the tail-pipe burner was in operation, the turbine-outlet temperatures listed in table I were calculated by means of the following relation:

$$H_6 = \frac{W_{a,3}H_{a,1} + \frac{W_{f,e}}{3600} h_{c,e}\eta_{b,e}}{W_{a,3} + \frac{W_{f,e}}{3600}} \tag{8}$$

1245

An engine combustion efficiency $\eta_{b,e}$ of approximately 98 percent at rated engine speed was determined from experiments with the standard-engine tail pipe and more complete temperature instrumentation. After calculation of turbine-outlet total enthalpy H_6 by equation (8), turbine-outlet temperature T_6 was determined from H_6 and fuel-air ratio f/a by the use of enthalpy-temperature charts.

Burner-inlet velocity. - Velocity at the burner-section inlet was calculated from the continuity equation by using static pressure measured at station 7, approximately $7\frac{1}{2}$ inches upstream of the flame holder, and assuming constant total pressure and total temperature from turbine outlet to burner inlet as follows:

$$V_7 = \frac{W_g}{\rho_7 g A_7} = \frac{W_g R T_6}{p_7 A_7}\left(\frac{p_7}{P_6}\right)^{\frac{\gamma_6-1}{\gamma_6}} \tag{9}$$

Combustion efficiency. - Tail-pipe combustion efficiency was obtained by dividing the enthalpy rise through the tail-pipe burner by the lower heating value of the tail-pipe fuel; dissociation of the exhaust gas was disregarded.

$$\eta_{b,t} = \frac{3600\ W_g \Delta H_t}{W_{f,t}h_{c,t}} = \frac{3600\ W_{a,3}H_a\Big]_1^9 + W_{f,e}H_{f,e}\Big]_m^9 - W_{f,e}h_{c,e} + W_{f,t}H_{f,t}\Big]_m^9}{W_{f,t}h_{c,t}} \tag{10}$$

The engine fuel was assumed to be completely burned in the engine; inasmuch as the engine combustion efficiency was found to be a approximately 98 percent, this assumption involves less than one-half of 1 percent error in the value of tail-pipe combustion efficiency. The enthalpy of the products of combustion was determined from the hydrogen-carbon ratio of the fuels by the method explained in reference 8.

Exhaust-gas total temperature. - The total temperature of the exhaust gas was calculated from exhaust-nozzle-outlet pressures and gas flow by means of the following equation:

$$T_9 = \frac{\gamma_9 g}{R}\left(\frac{C_d C_T A_9 p_9 M_9}{W_g}\right)^2 \left(\frac{P_8}{p_9}\right)^{\frac{\gamma_9-1}{\gamma_9}} \tag{11}$$

Exhaust-nozzle static pressure p_9 and outlet Mach number M_9 were determined by considering critical pressure ratio as follows:

When

$$\frac{P_8}{p_0} < \left(\frac{\gamma_9+1}{2}\right)^{\frac{\gamma_9}{\gamma_9-1}}$$

$$p_9 = p_0$$

and

$$M_9 = \sqrt{\frac{2}{\gamma_9-1}\left[\left(\frac{P_8}{p_0}\right)^{\frac{\gamma_9-1}{\gamma_9}} - 1\right]} \qquad \text{(subsonic flow)}$$

When

$$\frac{P_8}{p_0} > \left(\frac{\gamma_9+1}{2}\right)^{\frac{\gamma_9}{\gamma_9-1}}$$

$$p_9 = \frac{P_8}{\left(\frac{\gamma_9+1}{2}\right)^{\frac{\gamma_9}{\gamma_9-1}}}$$

and

$$M_9 = 1 \qquad \text{(sonic flow)}$$

The values of C_d and C_T for the exhaust nozzle used were determined from the following relations, which were experimentally obtained:

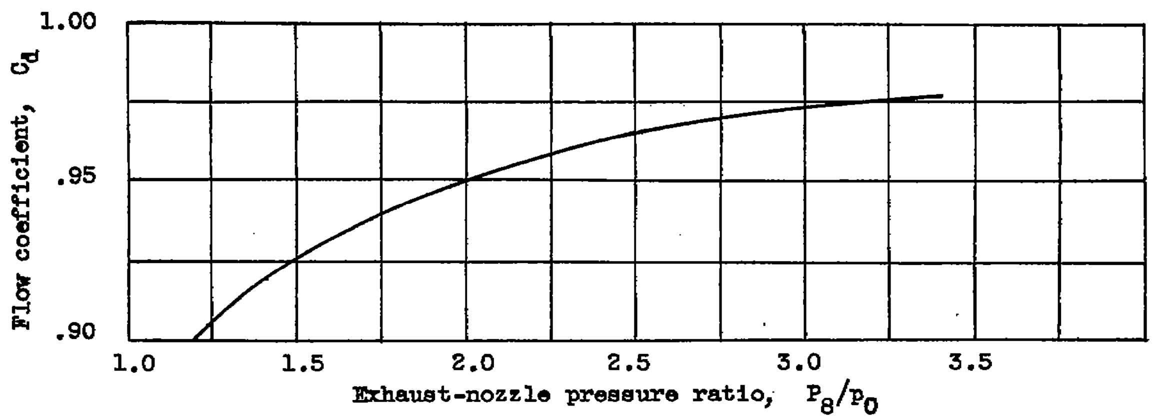

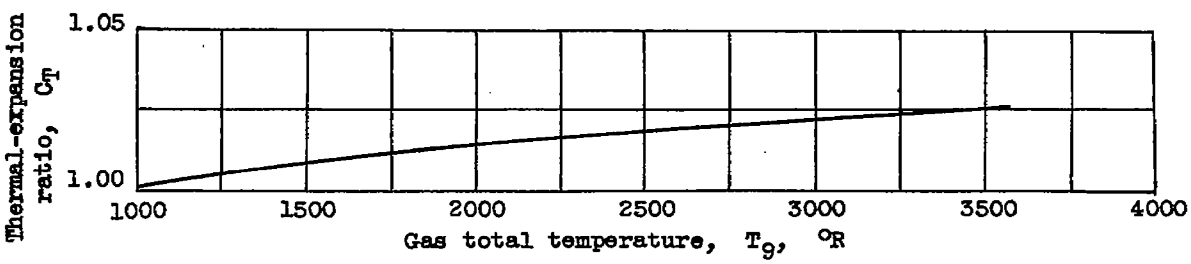

The ratio of specific heats γ_9 and the thermal-expansion ratio C_T were based on an estimated value of exhaust-gas temperature determined from the scale thrust measurement.

Augmented thrust. - Actual jet thrust was determined from the balance-scale measurements by use of the following equation:

$$F_{j,s} = B + D + D_r + \frac{W_{a,x}V_x}{g} + A_x(p_x - p_0) \tag{12}$$

The last two terms of this expression represent momentum and pressure forces on the installation at the slip joint in the inlet-air duct. External drag of the installation was determined from tests with an annular-shaped plug installed at the engine inlet to prevent air flow through the engine. Drag of the exhaust-nozzle survey rake was measured over a range of jet Mach numbers by a hydraulic-balance piston mechanism.

Equivalent free-stream momentum of the inlet air was subtracted from scale jet thrust to determine net thrust as follows:

$$F_n = F_{j,s} - \frac{W_{a,1}V_0}{g} \tag{13}$$

Normal thrust. - The augmented thrust ratio and engine specific fuel consumption were based on the net thrust obtainable at rated engine speed with the standard-engine tail pipe. In order to account for possible performance deterioration of the basic engine during the progress of the tail-pipe-burning program, the standard-engine thrust was calculated from measurements of total pressure and temperature at the turbine outlet, the gas flow leaving the turbine, and the total-pressure-loss ratio across the standard tail pipe, as shown in the following equation:

$$F_n = \frac{C_v\left(W_{a,3} + \frac{W_{f,e}}{3600}\right)}{g} \sqrt{\frac{2\gamma_6}{\gamma_6 - 1}\, gRT_6 \left[1 - \left(\frac{p_0}{P_8'}\right)^{\frac{\gamma_6 - 1}{\gamma_6}}\right]} - \frac{W_{a,1}V_0}{g} \tag{14}$$

Experimental data indicated that the total-pressure loss through the standard tail pipe from station 6 to station 8 was approximately 0.01 P_6 at rated engine speed. The total pressure $P_8{}'$ is therefore equal to 0.99 P_6. A nozzle-velocity coefficient C_v of 0.97 was used for the calculation of the results presented. This value of C_v was obtained from calibration tests of the engine with the standard-engine tail pipe and exhaust nozzle.

Rake jet thrust. - Jet thrust may be calculated from exhaust-nozzle-outlet pressure by assuming constant total pressure in the exhaust jet.

$$F_{j,9} = \frac{W_g}{g} V_j = \frac{W_g}{g} V_9 + C_d C_T A_9 (p_9 - p_0)$$

$$= C_d C_T A_9 \left[\gamma_9 p_9 M_9{}^2 + (p_9 - p_0)\right] \qquad (15)$$

The terms on the right side of equation (15) were determined in the same manner as for equation (11). Thus, the equation becomes for subsonic and sonic flows, respectively:

When

$$p_9 = p_0$$

$$F_{j,9} = C_d C_T A_9 \gamma_9 p_0 \quad \frac{2}{\gamma_9 - 1}\left[\left(\frac{P_8}{p_0}\right)^{\frac{\gamma_9 - 1}{\gamma_9}} - 1\right] \qquad (15a)$$

When

$$p_9 = \frac{P_8}{\left(\frac{\gamma_9 + 1}{2}\right)^{\frac{\gamma_9}{\gamma_9 - 1}}}$$

and

$$M_9 = 1$$

1245

$$F_{j,9} = C_d C_T A_9 \frac{P_8(\gamma_9+1)}{\left(\frac{\gamma_9+1}{2}\right)^{\frac{\gamma_9}{\gamma_9-1}}} - p_0 \qquad (15b)$$

Exhaust-nozzle velocity coefficient. - For the exhaust nozzle used, the velocity coefficient may be expressed as the ratio of scale jet thrust (equation (12)) to ideal jet thrust (equation (15)):

$$C_v = \frac{\text{actual } V_j}{\text{ideal } V_j} = \frac{F_{j,s}}{F_{j,9}}$$

The relation of the velocity coefficient with tail-pipe burning to nozzle pressure ratio is shown by the following curve, which was calculated from faired values of jet thrust:

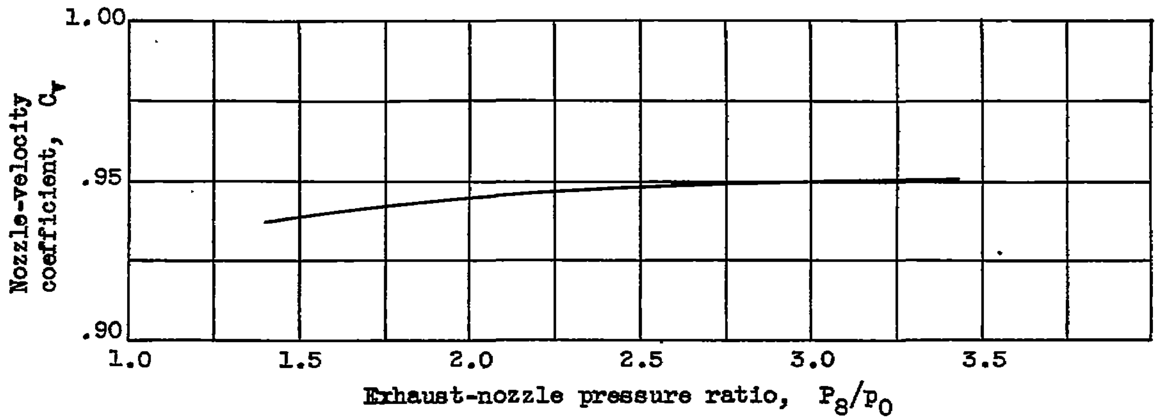

REFERENCES

1. Fleming, W. A., and Dietz, R. O., Jr.: Altitude-Wind-Tunnel Investigations of Thrust Augmentation of a Turbojet Engine. I - Performance with Tail-Pipe Burning. NACA RM E6I20, 1946.

2. Fleming, William A., and Golladay, Richard L.: Altitude-Wind-Tunnel Investigation of Thrust Augmentation of a Turbojet Engine. III - Performance with Tail-Pipe Burning in Standard-Size Tail Pipe. NACA RM E7F10, 1947. 1245

3. Fleming, William A., and Wallner, Lewis E.: Altitude-Wind-Tunnel Investigation of Tail-Pipe Burning with a Westinghouse X24C-4B Axial-Flow Turbojet Engine. NACA RM E8J25e, 1948.

4. Lundin, Bruce T., Dowman, Harry W., and Gabriel, David S.: Experimental Investigation of Thrust Augmentation of a Turbojet Engine at Zero Ram by Means of Tail-Pipe Burning. NACA RM E6J21, 1947.

5. Conrad, E. William, and Prince, William R.: Altitude Performance and Operational Characteristics of 29-Inch-Diameter Tail-Pipe Burner with Several Fuel Systems and Flame Holders on J35 Turbojet Engine. NACA RM E9G08, 1949.

6. Thorman, H. Carl, and Campbell, Carl E.: Altitude-Wind-Tunnel Investigation of Tail-Pipe Burner with Converging Conical Burner Section on J35-A-5 Turbojet Engine. NACA RM E9I16, 1950.

7. Breitwieser, Roland: Performance of a Ram-Jet-Type Combustor with Flame Holder Immersed in the Combustion Zone. NACA RM E8F21, 1948.

8. Turner, L. Richard, and Lord, Albert M.: Thermodynamic Charts for the Computation of Combustion and Mixture Temperatures at Constant Pressure. NACA TN 1086, 1946.

TABLE I - PERFORMANCE DATA

Run	Altitude (ft)	Flight Mach number M_0	Ambient pressure p_0 (lb/sq ft abs.)	Engine-inlet total pressure P_1 (lb/sq ft abs.)	Engine-inlet total temperature T_1 (°R)	Engine fuel flow $W_{f,e}$ (lb/hr)	Tail-pipe fuel flow $W_{f,t}$ (lb/hr)	Fuel distribution Stage 1	Stage 2	Stage 3	Jet thrust F_j (lb)	Net thrust F_n (lb)
Configuration A												
1	5,000	0.240	1753	1823	514	2381	2389	(a)	(a)	(a)	2829	2304
2	5,000	.240	1760	1831	511	2578	3293	—	—	—	3156	2626
3	5,000	.240	1756	1826	509	2795	4295	—	—	—	3583	3053
4	5,000	.265	1760	1849	509	2915	5376	—	—	—	3848	3268
5	5,000	.230	1767	1836	509	3181	7408	—	—	—	4072	3539
6	15,000	.525	1183	1427	488	2090	3193	—	—	—	3120	2241
7	15,000	.520	1193	1433	501	2200	4208	—	—	—	3220	2341
8	15,000	.525	1190	1430	502	2341	5685	—	—	—	3457	2582
9	15,000	.528	1190	1432	492	2520	7567	—	—	—	3703	2828
10	25,000	.260	781	819	466	1320	1986	—	—	—	1663	1407
11	25,000	.270	785	825	464	1447	3119	—	—	—	1897	1617
12	25,000	.270	781	821	470	1378	4577	—	—	—	1764	1488
13	25,000	.250	781	816	467	1251	6132	—	—	—	1617	1362
14	25,000	.260	781	819	466	1251	7388	—	—	—	1604	1348
15	25,000	.530	778	940	459	1475	2332	—	—	—	2151	1555
16	25,000	.525	781	939	464	1630	3073	—	—	—	2410	1819
17	25,000	.530	774	937	467	1728	4837	—	—	—	2584	1986
18	25,000	.525	774	933	463	1679	6172	—	—	—	2452	1864
19	25,000	.525	778	938	458	1572	7592	—	—	—	2360	1765
20	25,000	.730	771	1097	479	1475	1986	—	—	—	2383	1452
21	25,000	.725	788	1113	477	1768	3286	—	—	—	2862	1925
22	25,000	.725	778	1103	479	1825	4152	—	—	—	3000	2064
23	25,000	.725	774	1097	476	1962	5535	—	—	—	3189	2264
24	25,000	.730	771	1097	477	1933	6597	—	—	—	3142	2208
25	25,000	.725	788	1115	477	1943	7529	—	—	—	3170	2232
26	25,000	.920	785	1359	504	1533	1944	—	—	—	2931	1542
27	25,000	.920	792	1368	507	1816	3109	—	—	—	3348	1957
28	25,000	.910	796	1362	506	2060	4901	—	—	—	3812	2434
29	25,000	.920	771	1338	504	2150	6117	—	—	—	3881	2516
30	25,000	1.075	799	1653	529	2130	4450	—	—	—	4152	2270
31	25,000	1.075	788	1628	527	2410	6426	—	—	—	4589	2730
32	25,000	1.045	831	1656	530	2490	6948	—	—	—	(b)	(b)
33	25,000	1.050	810	1630	530	2481	7097	—	—	—	4690	2867
Configuration B												
1	5,000	0.245	1756	1832	503	2591	3032	(a)	(a)	(a)	2985	2447
2	5,000	.245	1760	1835	502	3031	4119	—	—	—	3761	3221
3	5,000	.240	1742	1812	506	3532	5635	—	—	—	4369	3840
4	5,000	.245	1732	1806	501	3727	6936	—	—	—	4789	4257
5	25,000	.280	788	833	468	1309	2436	—	—	—	1682	1401
6	25,000	.280	771	815	467	1766	3451	—	—	—	2195	1920
7	25,000	.720	778	1096	472	1369	1980	—	—	—	2128	1207
8	25,000	.730	774	1099	474	1943	3012	—	—	—	3060	2130
9	25,000	.710	788	1100	473	2291	4250	—	—	—	3545	2634
10	25,000	.920	781	1351	497	1698	2607	—	—	—	3117	1728
11	25,000	.925	774	1345	503	2319	3641	—	—	—	3998	2611
12	25,000	.920	781	1350	501	2620	5182	—	—	—	4528	3140
13	25,000	1.070	796	1635	518	1349	2772	—	—	—	2651	772
14	25,000	1.060	803	1631	518	1894	3559	—	—	—	3696	1841
15	25,000	1.075	781	1614	516	2894	5215	—	—	—	5251	3389
16	35,000	0.290	489	519	486	1020	3129	—	—	—	1139	958
Configuration C												
1	5,000	0.275	1752	1844	508	2710	3060	0.555	0.445	(c)	3205	2607
2	5,000	.275	1752	1846	505	2990	4080	.523	.478	—	3656	3050
3	5,000	.270	1755	1844	495	3190	4990	.545	.455	—	3995	3403
4	5,000	.270	1748	1838	501	3210	5030	.624	.376	—	3982	3394
5	5,000	.270	1748	1839	497	3210	5160	.419	.581	—	4035	3439
6	5,000	.270	1755	1844	509	3290	5940	.471	.529	—	4094	3508
7	5,000	.270	1752	1842	506	3590	7136	.521	.479	—	4551	3965
8	25,000	.270	782	823	456	1460	2320	.528	.472	—	1900	1626
9	25,000	.270	782	823	442	1750	3230	.519	.481	—	2304	2027
10	25,000	.275	779	820	445	1840	4170	.497	.503	—	2504	2226
11	25,000	.270	782	822	451	1880	5782	.505	.495	—	2524	2252
12	25,000	.925	782	1356	504	1750	2470	.483	.517	—	3161	1770
13	25,000	.925	782	1355	507	2150	3660	.502	.498	—	3836	2452
14	25,000	.910	786	1346	498	2470	5060	.504	.496	—	4249	2877
15	25,000	.920	782	1353	493	2670	6441	.529	.471	—	4564	3169
16	35,000	.265	497	522	450	1000	2050	.531	.469	—	1313	1144
17	35,000	.275	497	524	449	1080	2550	.531	.469	—	1427	1251
18	35,000	.280	490	517	450	1130	3090	.517	.483	—	1506	1331
19	35,000	.275	497	524	451	1130	3840	.508	.492	—	1529	1353

[a] Only total fuel flow was measured.

[b] Data unavailable.

[c] Two-stage flame holder.

NACA

[redacted]

1245

WITH TAIL-PIPE BURNING

Air flow W_a (lb/sec)	Specific fuel consumption W_f/F_n (lb/(hr) (lb thrust))	Total fuel-air ratio f/a	Tail-pipe fuel-air ratio $(f/a)_t$	Tail-pipe combustion efficiency $\eta_{b,t}$	Turbine-outlet total pressure P_6 (lb/sq ft abs.)	Turbine-outlet total temperature T_6 (°R)	Burner-section-inlet static pressure p_7 (lb/sq ft abs.)	Exhaust-nozzle total pressure P_9 (lb/sq ft abs.)	Exhaust-gas total temperature T_9 (°R)	Run
Configuration A										
62.93	2.070	0.0215	0.0107	0.582	2699	1269	2549	2552	1696	1
63.56	2.235	.0260	.0146	.602	2823	1310	2672	2673	1899	2
63.62	2.322	.0314	.0190	.629	2953	1375	2802	2797	2143	3
64.45	2.537	.0362	.0235	.554	3032	1398	2883	2871	2207	4
63.95	2.992	.0466	.0326	.504	3164	1478	3017	2998	2450	5
51.66	2.357	.0288	.0174	.624	2259	1295	2141	2133	2003	6
50.64	2.737	.0356	.0234	.563	2322	1359	2211	2194	2184	7
50.44	3,108	.0448	.0317	.485	2405	1418	2292	2272	2335	8
51.41	3.567	.0552	.0414	.384	2511	1454	2398	2350	2362	9
30.76	2.350	.0303	.0182	.552	1359	1319	1299	1284	1975	10
31.13	2.824	.0413	.0282	.479	1446	1385	1383	1372	2210	11
30.66	4.002	.0546	.0420	.257	1399	1355	1541	1311	1985	12
30.61	5.421	.0678	.0563	.138	1331	1278	1271	1241	1676	13
30.76	6.409	.0789	.0675	.110	1328	1270	1264	1246	1643	14
35.74	2.448	.0299	.0183	.575	1543	1279	1468	1455	1973	15
35.44	2.585	.0373	.0244	.551	1633	1374	1559	1539	2215	16
35.15	3.306	.0526	.0388	.393	1679	1428	1605	1580	2315	17
35.26	4.212	.0627	.0493	.276	1648	1406	1577	1551	2158	18
35.71	5.192	.0722	.0598	.187	1604	1329	1528	1504	1930	19
40.31	2.384	.0241	.0138	.573	1638	1211	1542	1534	1752	20
41.04	2.625	.0346	.0225	.568	1827	1327	1735	1729	2157	21
40.54	2.896	.0415	.0288	.517	1878	1369	1789	1774	2281	22
40.51	3.311	.0521	.0385	.431	1947	1420	1862	1828	2386	23
40.44	3.863	.0594	.0459	.331	1919	1417	1827	1798	2272	24
41.10	4.244	.0649	.0516	.291	1945	1406	1851	1823	2231	25
47.78	2.255	.0204	.0114	.587	1846	1150	1750	1728	1618	26
47.83	2.517	.0289	.0182	.538	2011	1269	1894	1887	1906	27
47.71	2.860	.0410	.0289	.476	2175	1355	2067	2034	2195	28
46.94	3.286	.0496	.0367	.372	2173	1408	2077	2022	2206	29
55.56	2.899	.0333	.0225	.546	2414	1290	2281	2275	2075	30
54.89	3.237	.0452	.0329	.451	2531	1389	2397	2377	2277	31
55.53	(c)	.0478	.0352	(c)	(c)	1407	(c)	(c)	(c)	32
54.67	3.341	.0493	.0365	.450	2591	1421	2461	2433	2383	33
Configuration B										
64.51	2.298	0.0244	0.0132	0.570	2838	1295	2678	2680	1805	1
64.75	2.220	.0311	.0179	.826	3171	1424	3034	2986	2365	2
63.48	2.387	.0407	.0250	.782	3348	1585	3192	3150	2755	3
63.83	2.505	.0472	.0307	.696	3454	1634	3316	3241	2869	4
31.20	2.673	.0337	.0219	.517	1420	1303	1348	1336	2017	5
30.57	2.717	.0482	.0319	.591	1586	1589	1521	1497	2680	6
40.79	2.775	.0230	.0136	.390	1570	1150	1475	1475	1519	7
40.73	2.326	.0342	.0208	.706	1920	1413	1830	1815	2336	8
40.81	2.483	.0452	.0294	.752	2134	1563	2052	2022	2859	9
48.10	2.491	.0251	.0152	.494	1942	1205	1827	1825	1718	10
47.37	2.283	.0354	.0216	.767	2296	1460	2182	2160	2487	11
47.74	2.485	.0461	.0306	.683	2464	1570	2362	2322	2793	12
56.34	5.338	.0205	.0138	.084	1814	1003	1680	1705	1084	13
56.21	2.962	.0272	.0178	.384	2203	1190	2077	2078	1643	14
55.54	2.393	.0412	.0265	.742	2805	1551	2675	2639	2709	15
18.53	4.331	.0631	.0476	.304	933	1556	901	871	2337	16
Configuration C										
64.36	2.213	0.0252	0.0134	0.675	2856	1339	2727	2742	1945	1
64.80	2.318	.0307	.0177	.693	3026	1414	2900	2892	2197	2
65.85	2.404	.0349	.0213	.660	3167	1440	2976	3005	2322	3
64.99	2.428	.0357	.0218	.667	3157	1469	3027	2997	2369	4
65.43	2.434	.0360	.0222	.667	3173	1459	3039	3017	2375	5
64.23	2.631	.0405	.0261	.623	3198	1509	3073	3044	2487	6
64.52	2.705	.0469	.0312	.629	3363	1585	3232	3192	2726	7
31.48	2.325	.0338	.0207	.654	1485	1378	1404	1397	2229	8
32.21	2.457	.0436	.0283	.689	1665	1507	1585	1563	2668	9
31.93	2.700	.0532	.0369	.605	1714	1573	1634	1606	2839	10
31.71	3.402	.0682	.0515	.454	1732	1604	1663	1627	2852	11
47.68	2.384	.0248	.0145	.755	2006	1235	1907	1924	1969	12
47.37	2.369	.0345	.0217	.729	2235	1403	2134	2118	2395	13
47.84	2.617	.0444	.0298	.669	2407	1509	2304	2281	2692	14
48.48	2.875	.0530	.0375	.637	2567	1563	2461	2425	2925	15
19.89	2.666	.0432	.0290	.546	978	1440	930	919	2393	16
20.00	2.902	.0512	.0360	.498	1022	1503	973	957	2542	17
19.71	3.171	.0605	.0443	.480	1050	1570	1003	986	2745	18
19.95	3.673	.0703	.0543	.377	1056	1560	1009	991	2649	19

NACA

[redacted]

1245

TABLE I - PERFORMANCE DATA WITH

Run	Altitude (ft)	Flight Mach number M_0	Ambient pressure p_0 (lb/sq ft abs.)	Engine-inlet total pressure P_1 (lb/sq ft abs.)	Engine-inlet total temperature T_1 (°R)	Engine fuel flow $W_{f,e}$ (lb/hr)	Tail-pipe fuel flow $W_{f,t}$ (lb/hr)	Fuel distribution			Jet thrust F_j (lb)	Net thrust F_n (lb)
								Stage 1	Stage 2	Stage 3		
Configuration D												
1	5,000	0.275	1759	1853	497	2345	3000	0.673	0.246	0.081	2340	1734
2	5,000	.265	1752	1840	498	2610	4000	.684	.219	.097	2856	2271
3	5,000	.275	1752	1847	510	3330	4900	.713	.203	.084	4072	3468
4	5,000	.275	1752	1845	510	3330	4950	.658	.196	.146	4125	3527
5	5,000	.275	1752	1847	508	3330	5040	.667	.247	.086	4037	3432
6	5,000	.285	1752	1855	505	3560	5850	.677	.179	.144	4395	3761
7	5,000	.270	1755	1845	510	3230	4970	.424	.417	.159	3841	3256
8	5,000	.265	1752	1840	515	3350	4980	.656	.143	.201	4063	3485
9	5,000	.270	1755	1846	510	3290	4990	.353	.553	.094	4059	3467
10	5,000	.280	1752	1848	510	3300	4990	.543	.270	.187	4079	3471
11	5,000	.275	1752	1845	505	3330	5020	.595	.247	.158	4073	3473
12	5,000	.270	1752	1843	505	3250	5040	.481	.437	.082	3913	3320
13	5,000	.275	1752	1845	501	3270	5080	.521	.425	.054	3983	3381
14	5,000	.275	1752	1844	515	3320	5080	.500	.254	.246	4045	3451
15	10,000	.250	1452	1515	501	2560	3250	.698	.155	.147	3090	2644
16	10,000	.260	1445	1516	486	2860	4200	.617	.247	.136	3523	3042
17	10,000	.250	1452	1516	499	2930	4700	.645	.232	.123	3612	3160
18	10,000	.265	1452	1524	491	3070	5180	.624	.244	.132	3825	3338
19	10,000	.260	1449	1519	495	3150	5835	.620	.257	.123	3952	3478
20	15,000	.280	1188	1254	485	2270	3270	.609	.228	.163	2841	2416
21	15,000	.270	1188	1250	467	2480	3910	.666	.203	.131	3116	2702
22	15,000	.280	1188	1254	474	2670	4550	.686	.197	.117	3432	3004
23	15,000	.260	1188	1245	480	2700	4970	.671	.203	.126	3510	3117
24	15,000	.265	1188	1248	483	2770	5290	.665	.220	.115	3499	3094
25	25,000	.280	782	825	444	1660	2400	.627	.243	.130	2122	1838
26	25,000	.285	782	827	447	1830	3050	.644	.226	.130	2339	2047
27	25,000	.275	782	824	451	1900	3530	.654	.214	.132	2462	2181
28	25,000	.280	782	826	453	1980	4080	.631	.217	.152	2532	2246
29	25,000	.920	782	1356	486	1340	2630	.623	.240	.137	2283	874
30	25,000	.920	779	1346	497	2090	3080	.651	.233	.116	3565	2183
31	25,000	.920	782	1351	501	2400	3950	.687	.234	.079	4068	2685
32	25,000	.915	775	1331	496	2570	4500	.650	.197	.153	4257	2896
33	25,000	.920	775	1339	481	2700	4970	.643	.254	.103	4511	3120
34	35,000	.250	497	519	499	680	1650	.614	.298	.088	672	518
35	35,000	.315	497	531	494	970	2000	.635	.247	.118	1160	967
36	35,000	.325	493	530	496	1055	2450	.565	.279	.156	1279	1077
37	35,000	.290	490	519	496	1060	2800	.531	.303	.166	1251	1075
38	40,000	.235	385	400	504	740	1500	.526	.319	.155	836	726
39	40,000	.225	385	399	503	780	1750	.568	.272	.160	903	798
40	40,000	.240	385	401	503	830	2170	.597	.235	.169	986	872
Configuration E												
1	5,000	0.270	1752	1843	498	2450	3070	[d]0.608	[e]0.392		2694	2097
2	5,000	.275	1759	1855	510	2600	3550	.761	.239		2930	2330
3	5,000	.285	1752	1854	499	2660	4040	.770	.230		3072	2438
4	5,000	.265	1748	1836	511	2910	4480	.771	.229		3419	2841
5	5,000	.275	1759	1853	504	3210	5110	.763	.237		3856	3253
6	5,000	.280	1752	1848	504	3430	5540	.760	.240		4233	3622
7	5,000	.245	1794	1872	511	3590	6045	.685	.315		4399	3852
8	25,000	.920	775	1338	499	1900	3050	.772	.228		3331	1959
9	25,000	.925	789	1376	505	2120	3540	.760	.240		4003	2586
10	25,000	.910	782	1338	493	1960	3610	.763	.237		3369	2001
11	25,000	.915	775	1336	502	2320	4060	.755	.245		3951	2585
12	35,000	.275	490	516	463	670	1510	.758	.242		689	518
13	35,000	.265	497	522	465	700	1670	.716	.284		675	507
14	35,000	.275	490	516	465	1005	1730	.783	.217		1223	1053
15	35,000	.265	493	518	465	700	1730	.769	.231		726	559
16	35,000	.265	497	522	466	1105	1850	.760	.240		1348	1180
17	35,000	.280	490	517	465	1140	2010	.769	.231		1387	1214
18	35,000	.280	490	517	464	1220	2110	.754	.246		1421	1247

[d]Fuel-injector bars.

[e]Fuel supply to stages 2 and 3 combined.

TAIL-PIPE BURNING - Concluded

Air flow W_a (lb/sec)	Specific fuel consumption W_f/F_n (lb/(hr)(lb thrust))	Total fuel-air ratio f/a	Tail-pipe fuel-air ratio $(f/a)_t$	Tail-pipe combustion efficiency $\eta_{b,t}$	Turbine-outlet total pressure P_6 (lb/sq ft abs.)	Turbine-outlet total temperature T_6 (°R)	Burner-section-inlet static pressure p_7 (lb/sq ft abs.)	Exhaust-nozzle total pressure P_9 (lb/sq ft abs.)	Exhaust-gas total temperature T_9 (°R)	Run
Configuration D										
65.92	3.082	0.0228	0.0128	0.284	2636	1214	2512	2544	1470	1
65.34	2.911	.0284	.0172	.490	2834	1289	2713	2727	1847	2
64.20	2.373	.0361	.0215	.817	3248	1520	3120	3082	2598	3
64.14	2.348	.0364	.0218	.841	3268	1520	3141	3107	2641	4
64.44	2.439	.0366	.0220	.807	3272	1516	3142	3100	2604	5
64.97	2.502	.0409	.0254	.788	3397	1575	3274	3222	2767	6
64.14	2.518	.0360	.0218	.764	3212	1494	3083	3043	2518	7
63.41	2.390	.0370	.0221	.860	3265	1547	3139	3105	2698	8
64.20	2.388	.0363	.0219	.780	3234	1509	3104	3061	2552	9
64.25	2.388	.0364	.0219	.786	3237	1516	3115	3074	2571	10
64.71	2.404	.0364	.0219	.775	3234	1513	3112	3079	2549	11
64.66	2.497	.0362	.0220	.718	3203	1490	3072	3033	2462	12
65.19	2.470	.0361	.0220	.721	3228	1478	3097	3053	2462	13
63.52	2.434	.0372	.0225	.800	3245	1531	3117	3075	2629	14
53.53	2.197	.0306	.0171	.767	2555	1439	2448	2420	2273	15
54.97	2.321	.0362	.0215	.746	2740	1505	2626	2584	2494	16
53.74	2.415	.0401	.0247	.713	2759	1560	2646	2597	2624	17
54.80	2.472	.0425	.0267	.716	2855	1577	2742	2692	2712	18
54.24	2.583	.0468	.0304	.693	2895	1621	2784	2732	2846	19
45.55	2.293	.0342	.0202	.733	2225	1461	2125	2092	2386	20
46.89	2.365	.0384	.0235	.690	2334	1504	2230	2200	2492	21
46.48	2.403	.0438	.0276	.715	2439	1594	2339	2294	2759	22
45.67	2.461	.0474	.0307	.701	2454	1632	2350	2305	2873	23
45.55	2.605	.0500	.0328	.691	2487	1662	2385	2339	2958	24
32.15	2.209	.0356	.0210	.744	1587	1463	1511	1485	2438	25
32.06	2.384	.0430	.0269	.761	1688	1561	1613	1581	2779	26
31.77	2.490	.0483	.0314	.744	1732	1617	1656	1621	2962	27
31.71	2.698	.0541	.0364	.707	1779	1669	1704	1665	3108	28
49.19	4.542	.0226	.0150	.238	1707	1040	1599	1622	1289	29
47.89	2.368	.0304	.0181	.793	2200	1361	2102	2082	2280	30
47.75	2.365	.0375	.0233	.855	2387	1488	2292	2264	2701	31
47.43	2.441	.0421	.0268	.853	2479	1552	2382	2341	2911	32
49.05	2.458	.0441	.0286	.887	2624	1552	2514	2473	3042	33
18.13	4.498	.0361	.0256	.113	749	1250	703	707	1428	34
18.72	3.071	.0447	.0301	.539	940	1510	895	885	2471	35
18.63	3.254	.0531	.0371	.532	985	1595	938	925	2715	36
18.23	3.591	.0598	.0434	.426	961	1620	914	900	2636	37
13.75	3.085	.0460	.0308	.499	699	1552	662	654	2454	38
13.73	3.170	.0520	.0360	.494	719	1602	682	674	2616	39
13.79	3.440	.0615	.0445	.455	748	1663	712	699	2764	40
Configuration E										
65.50	2.632	0.0237	0.0132	0.439	2749	1245	2602	2617	1643	1
64.42	2.639	.0268	.0155	.463	2824	1305	2674	2670	1787	2
65.79	2.748	.0287	.0173	.411	2848	1300	2705	2699	1774	3
63.72	2.601	.0326	.0198	.561	2988	1407	2833	2815	2108	4
65.14	2.558	.0360	.0221	.658	3193	1472	3037	3012	2377	5
64.97	2.477	.0389	.0240	.709	3330	1538	3170	3107	2562	6
65.02	2.501	.0418	.0262	.743	3435	1587	3270	3217	2741	7
47.48	2.527	.0292	.0180	.597	2049	1289	1952	1935	1996	8
48.29	2.189	.0329	.0206	.652	2207	1370	2094	2076	2215	9
47.97	2.784	.0326	.0211	.529	2091	1304	1988	1973	2019	10
47.12	2.468	.0382	.0243	.741	2335	1469	2218	2185	2570	11
19.23	4.208	.0318	.0220	.050	725	1170	682	696	1236	12
19.36	4.675	.0343	.0242	.107	752	1189	709	722	1352	13
19.13	2.597	.0403	.0255	.628	944	1493	901	895	2466	14
19.21	4.347	.0355	.0253	.094	746	1192	703	715	1343	15
19.32	2.504	.0431	.0270	.706	994	1576	952	945	2707	16
19.17	2.595	.0464	.0296	.662	1003	1621	958	949	2762	17
19.23	2.670	.0489	.0310	.679	1030	1689	987	975	2897	18

NACA

[redacted]

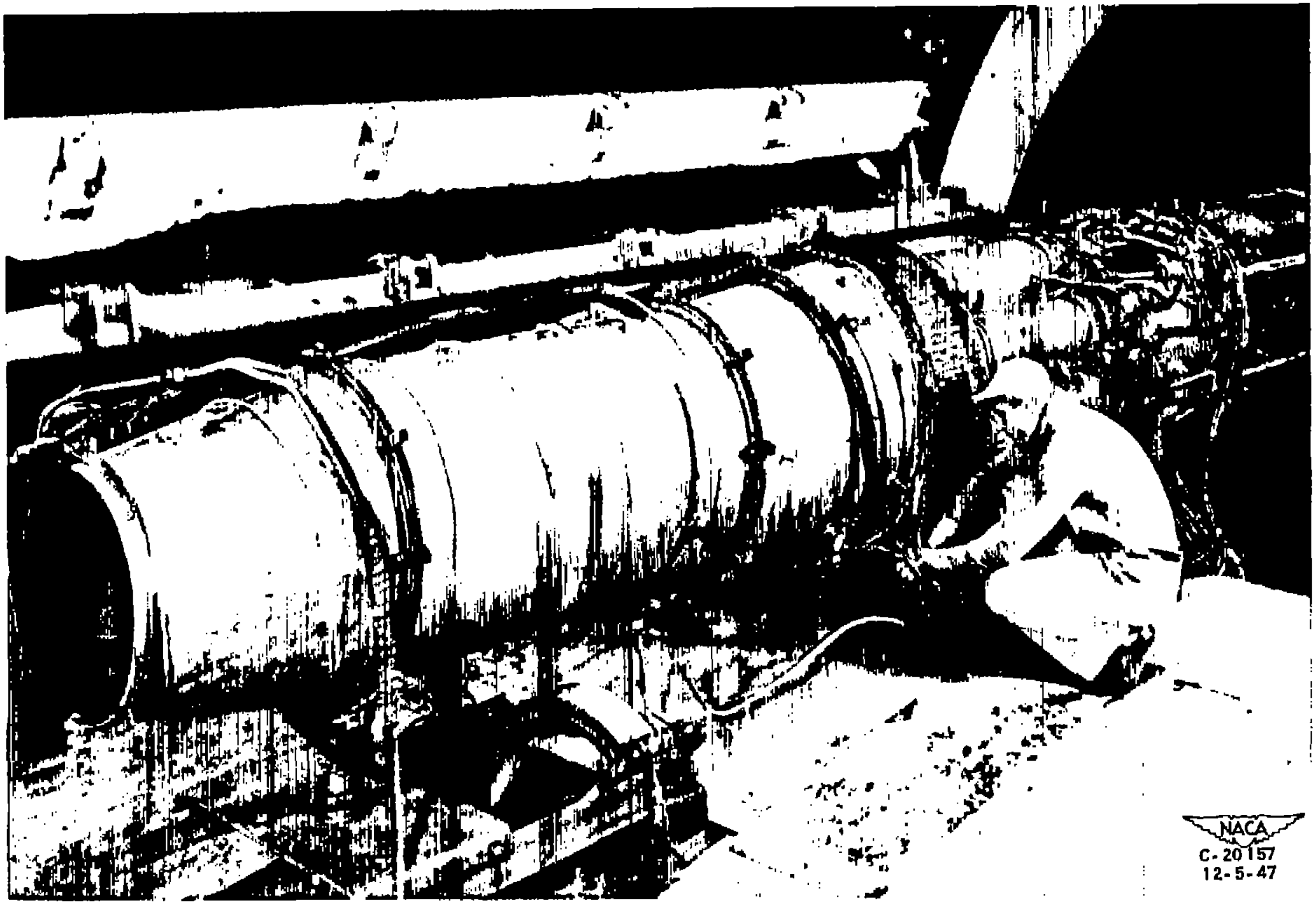

Figure 1. - Installation of J35-A-5 turbojet engine and tail-pipe burner in altitude wind tunnel.

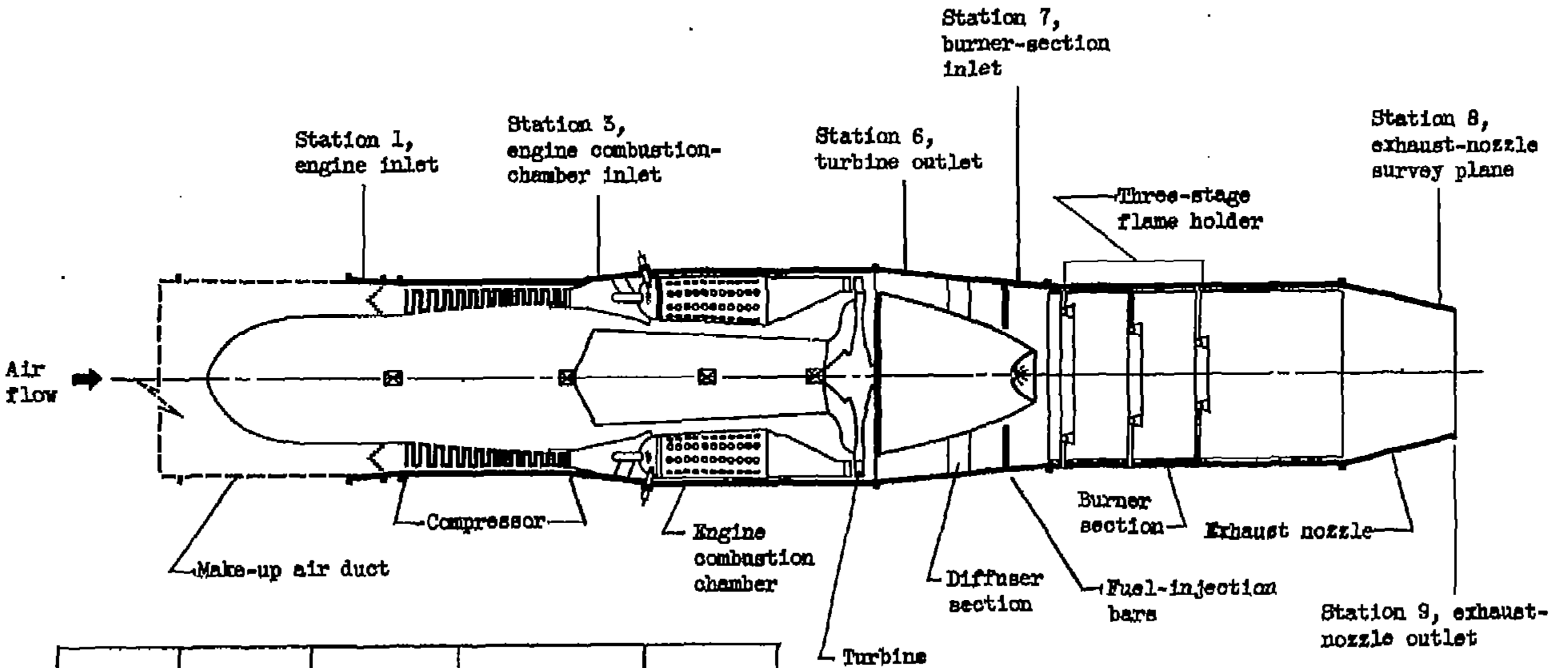

Station	Total-pressure tubes	Static-pressure tubes	Wall static-pressure orifices	Thermo-couples
1	6	4		4
6	20		2	16
7		2	3	
8	8		6	

Figure 2. - Cross section of tail-pipe-burner installation showing stations at which instrumentation was installed.

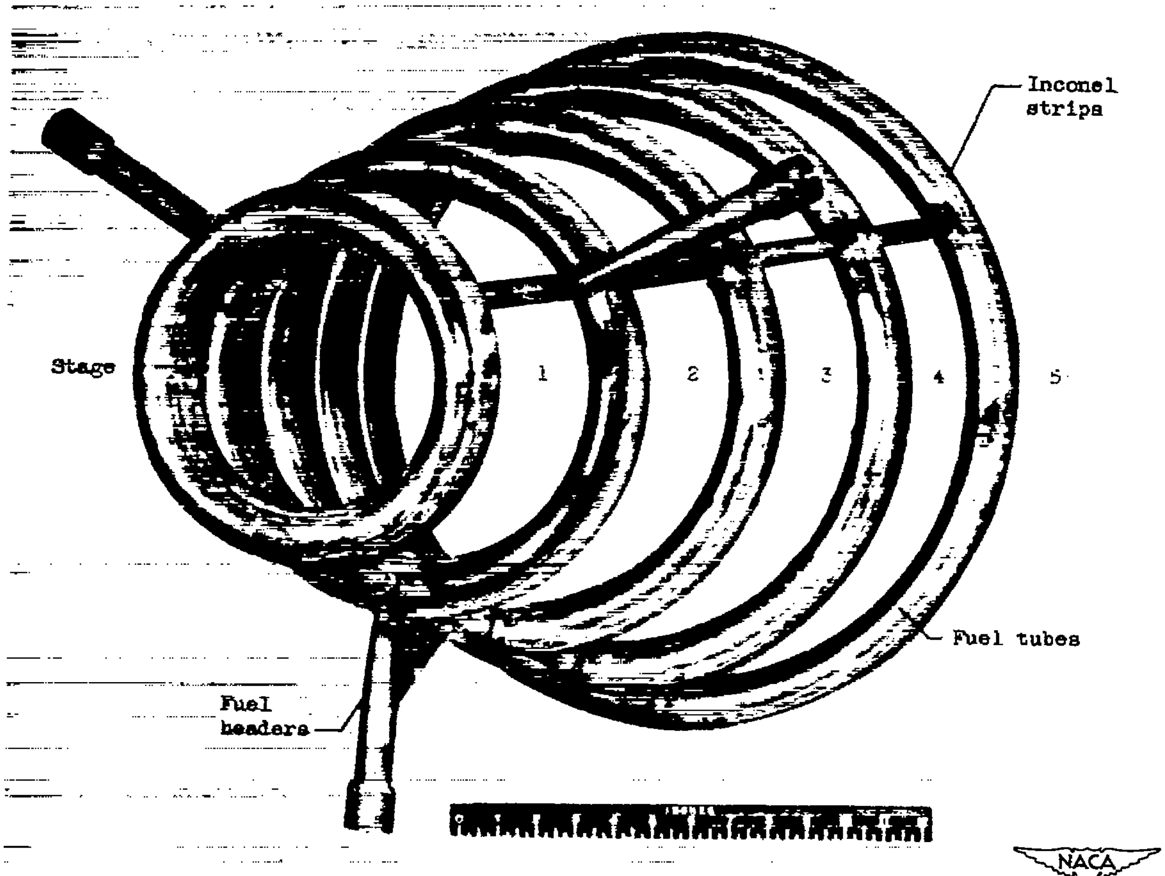

Figure 3. - Five-stage flame holder used with configuration A.

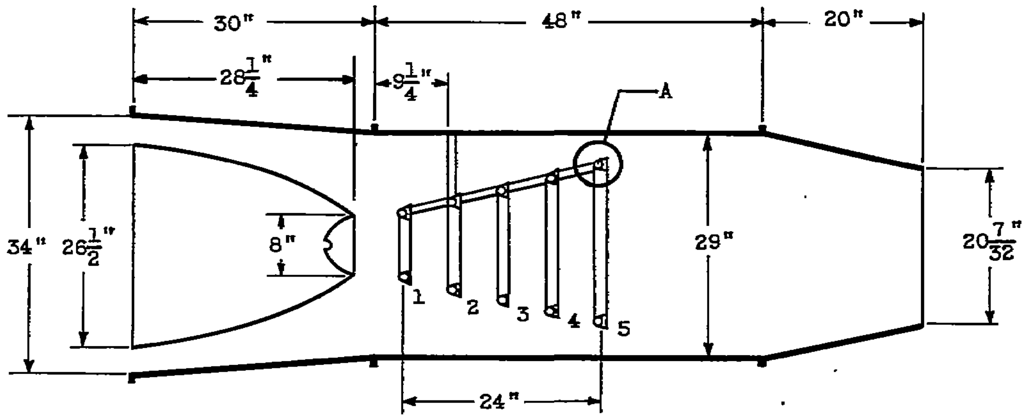

Description of fuel tubes

Stage	1	2	3	4	5
Diam. at center line	$8\frac{1}{2}$	$11\frac{9}{16}$	$14\frac{5}{8}$	$17\frac{11}{16}$	$20\frac{1}{4}$
Jets upstream	5	10	14	20	24
Jets downstream	0	5	7	10	12

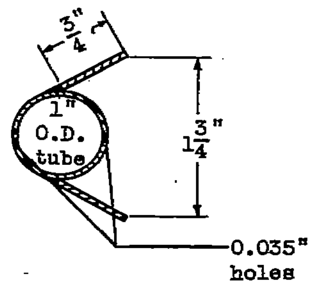

Detail A

(a) Configuration A.

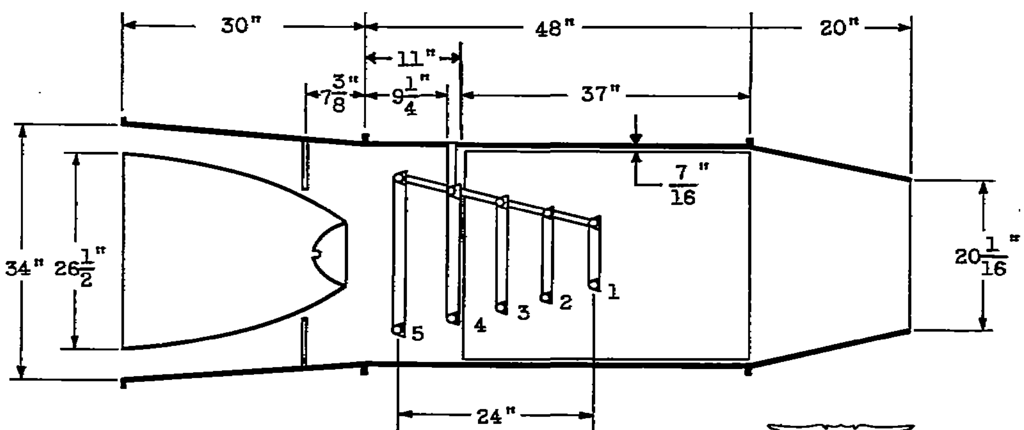

(b) Configuration B.

Figure 4. - Diagrammatic sketches of tail-pipe-burner assembly.

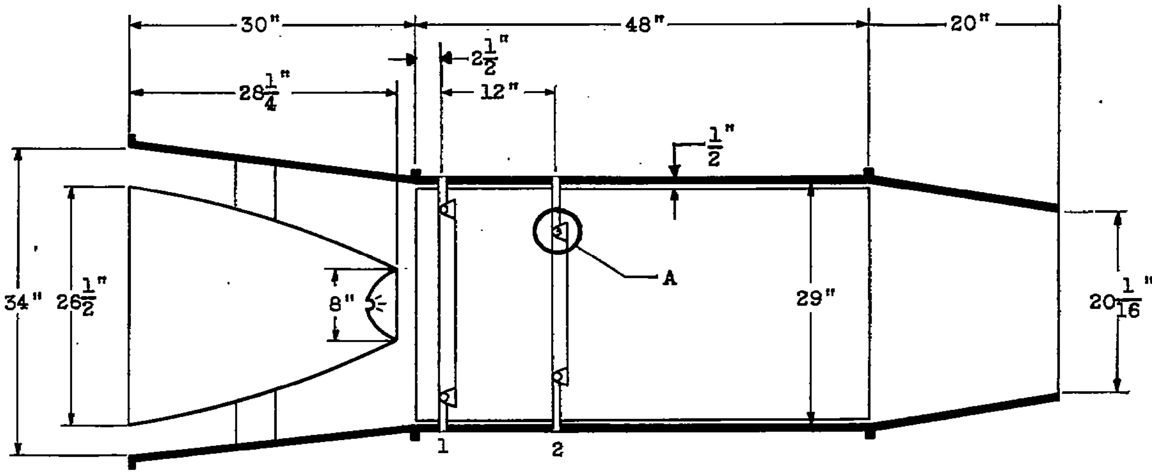

Description of fuel tubes

Stage	1	2
Diam. at center line	21	$16\frac{3}{4}$
Jets upstream	52	28
Jets at 45°	0	14

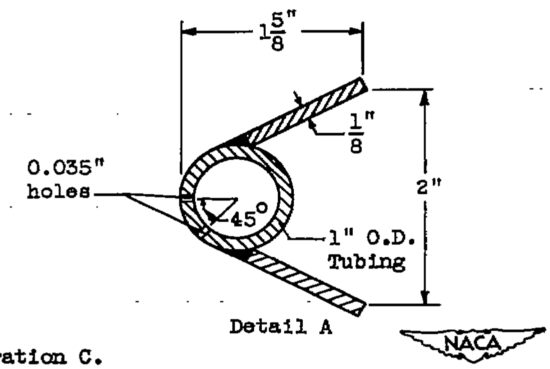

(c) Configuration C.

Figure 4. - Continued. Diagrammatic sketches of tail-pipe-burner assembly.

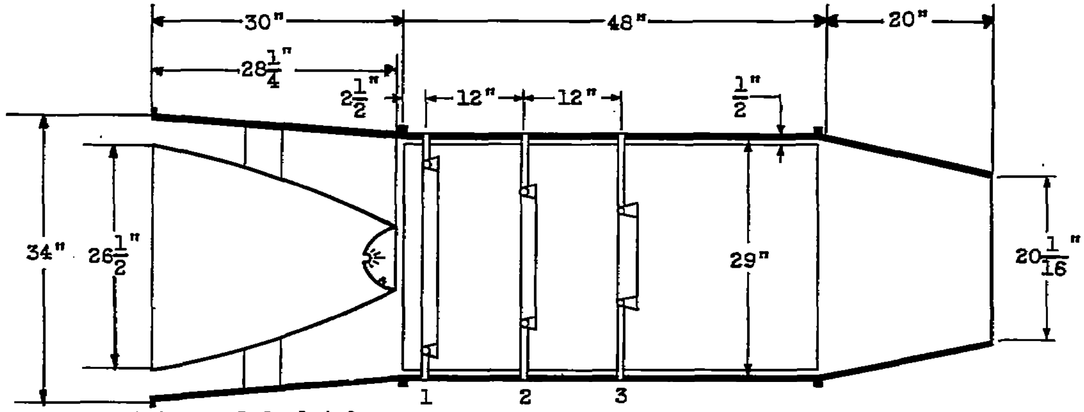

Description of fuel tubes

Stage	1	2	3
Diam. at center line	$22\frac{7}{8}$	$16\frac{3}{4}$	$11\frac{1}{2}$
Jets upstream	52	28	20

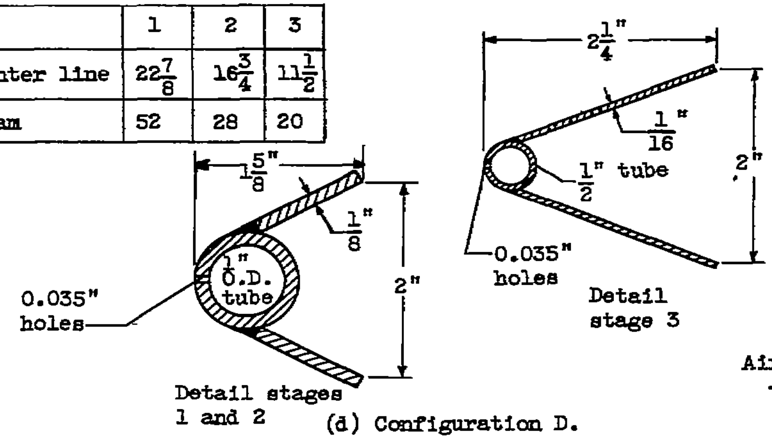

(d) Configuration D.

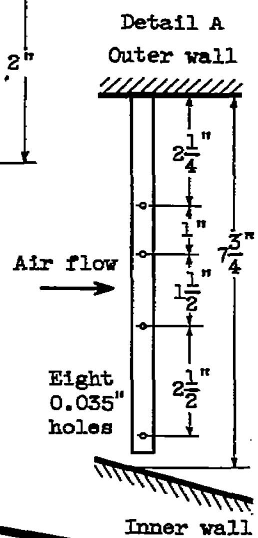

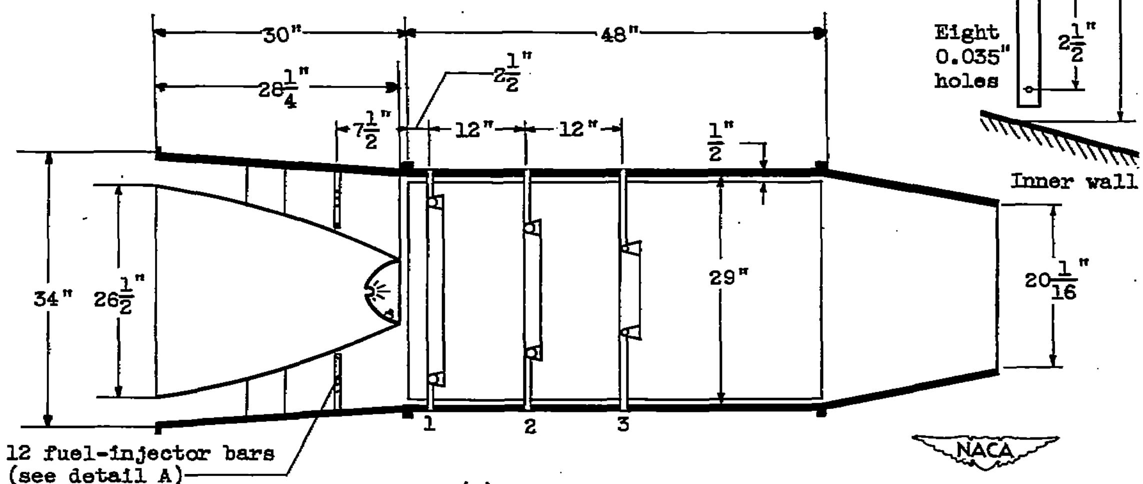

(e) Configuration E.

Figure 4. - Concluded. Diagrammatic sketches of tail-pipe-burner assembly.

[redacted]

1245

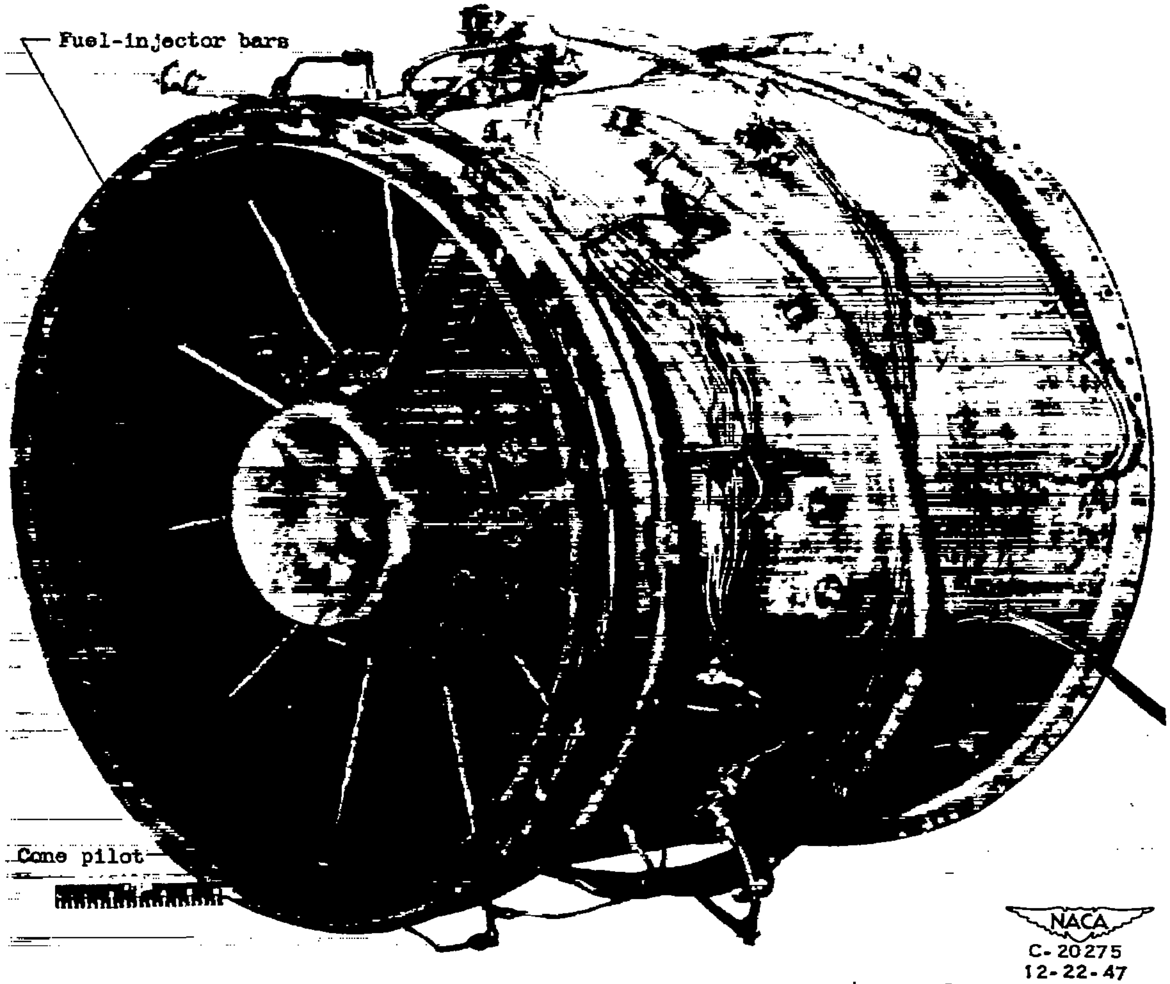

Figure 5. - Diffuser section with cone pilot and fuel-injector bars used with configurations B and E.

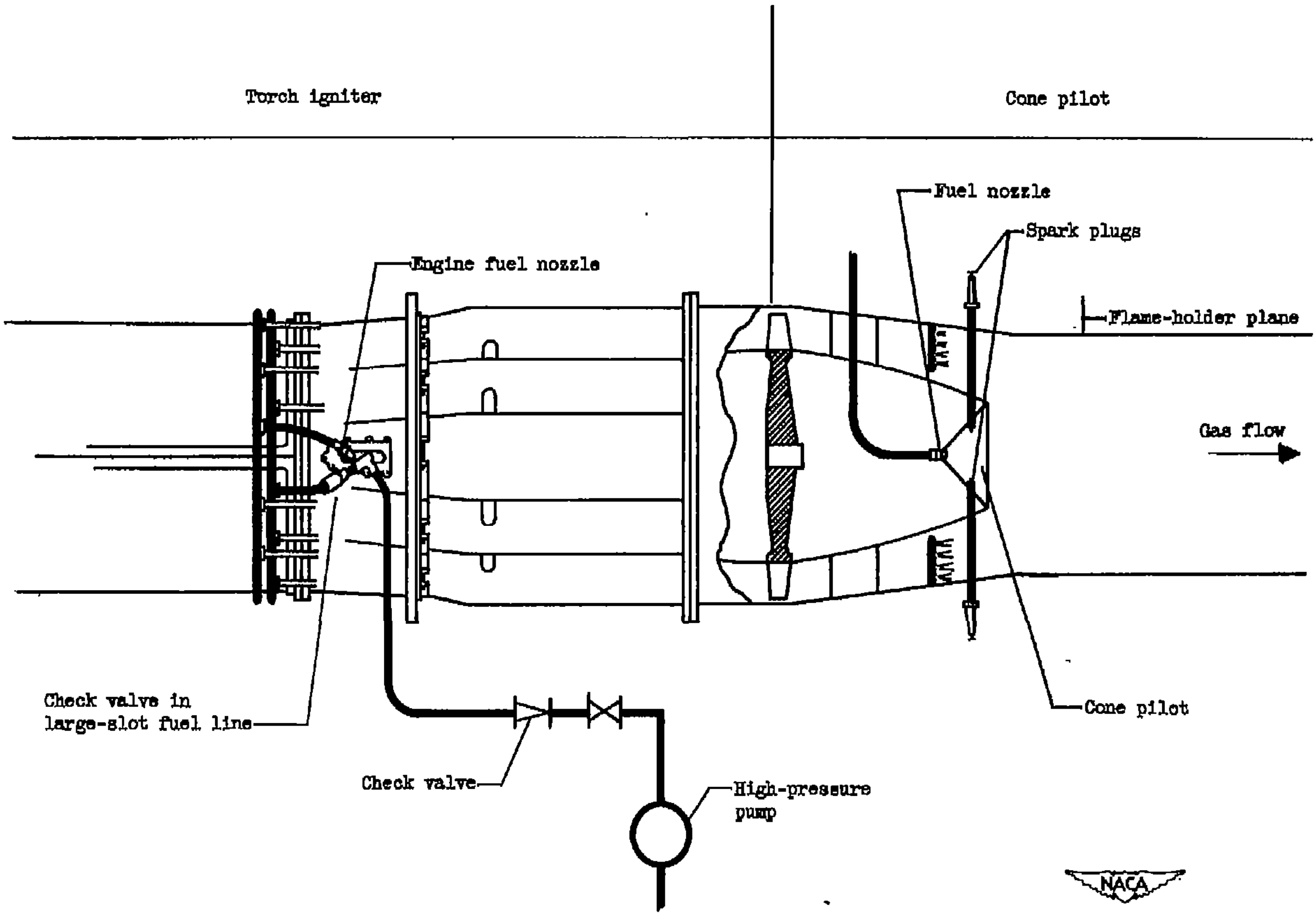

Figure 6. - Diagrammatic sketch of ignition systems.

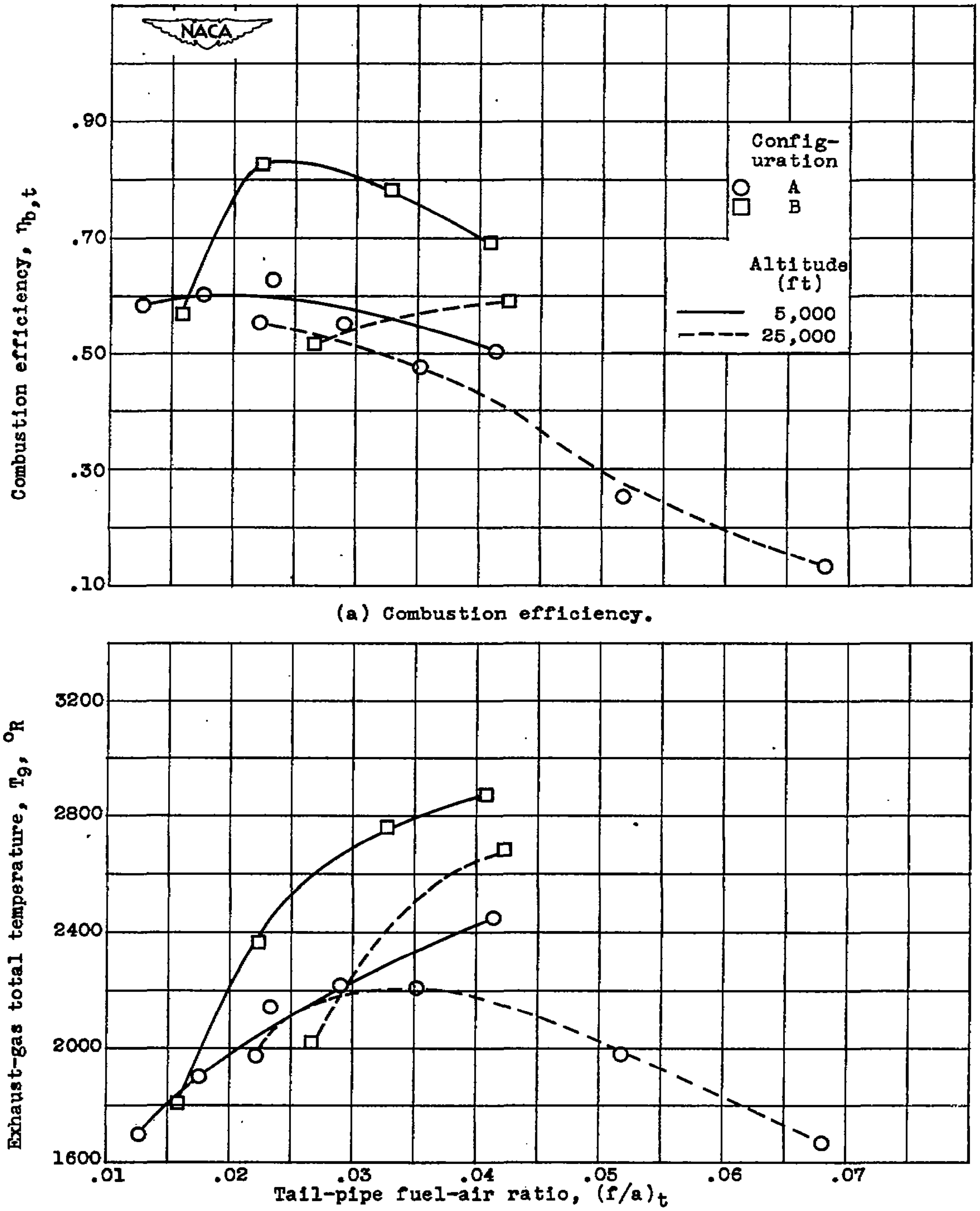

(a) Combustion efficiency.

(b) Exhaust-gas total temperature.

Figure 7. - Effect of flame-holder design on variation of exhaust-gas total temperature and combustion efficiency with tail-pipe fuel-air ratio. Flight Mach number, 0.27.

1245

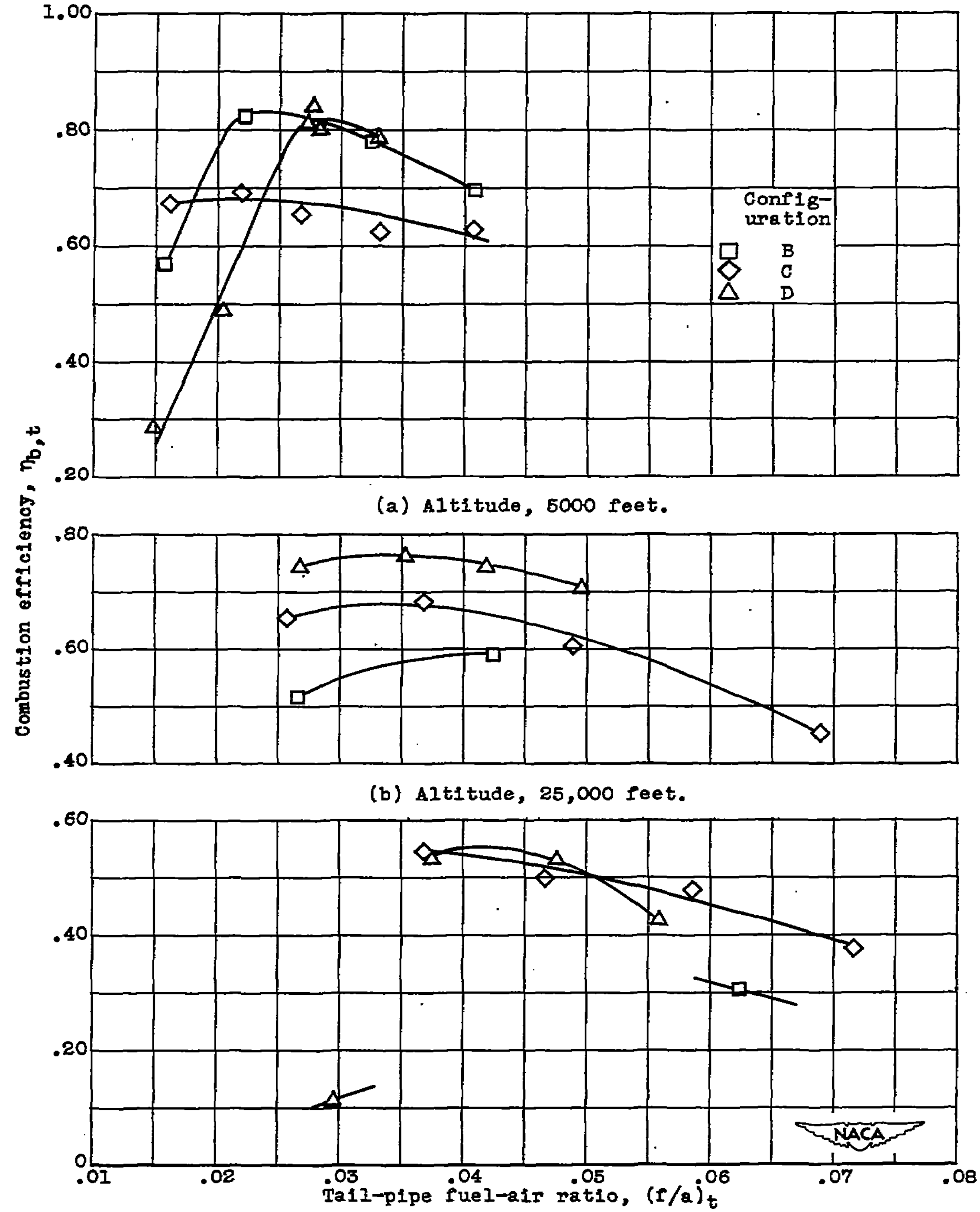

(a) Altitude, 5000 feet.

(b) Altitude, 25,000 feet.

(c) Altitude, 35,000 feet.

Figure 8. - Effect of altitude on variation of combustion efficiency with tail-pipe fuel-air ratio for configurations B, C, and D. Flight Mach number, 0.27.

[redacted]

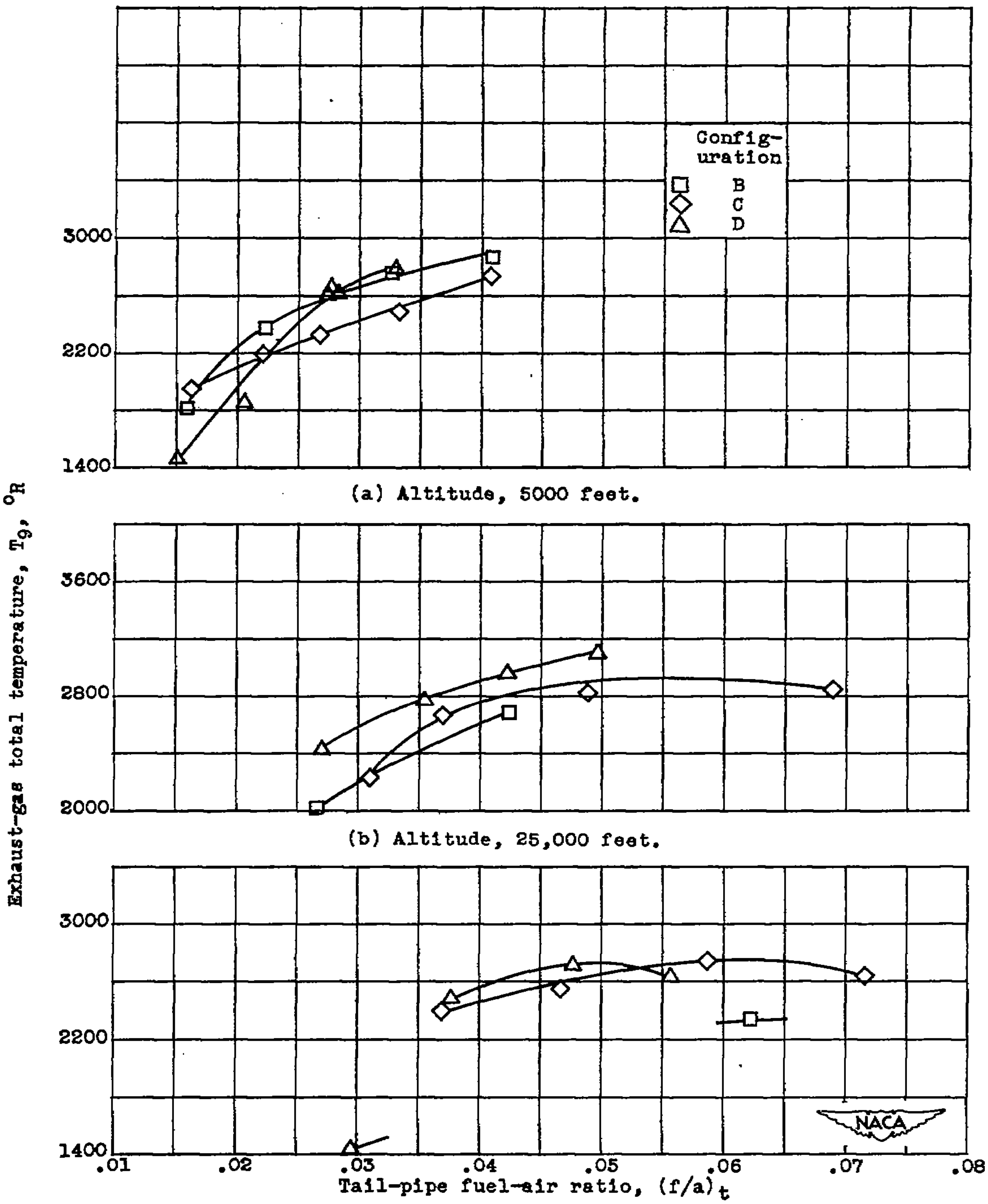

(c) Altitude, 35,000 feet.

Figure 9. - Effect of altitude on variation of exhaust-gas total temperature with tail-pipe fuel-air ratio for configurations B, C, and D. Flight Mach number, 0.27.

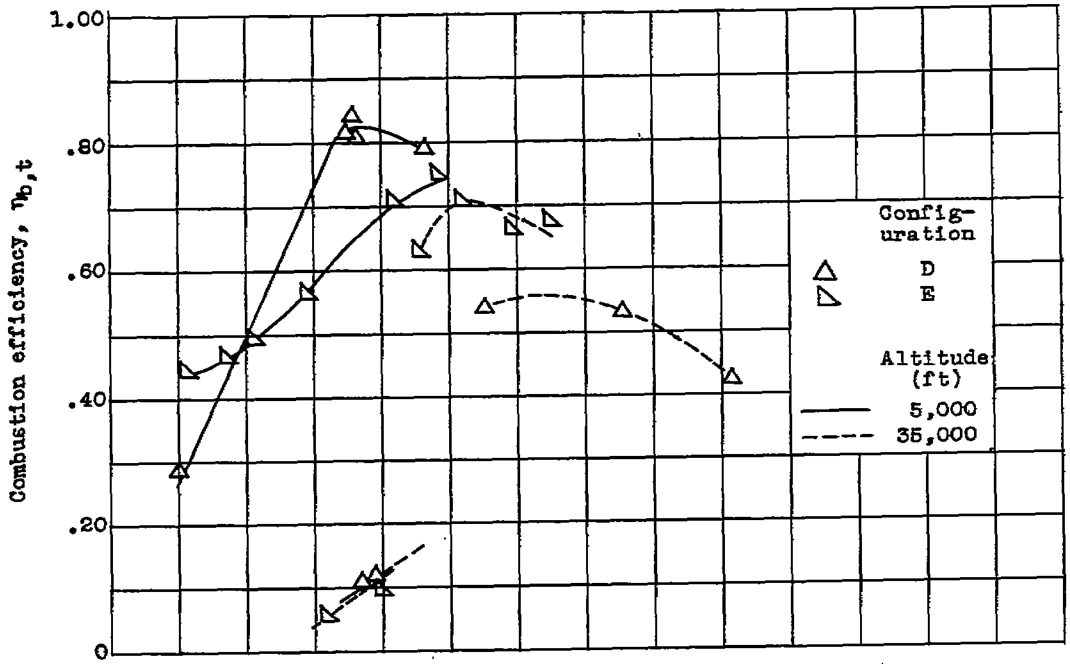

(a) Combustion efficiency.

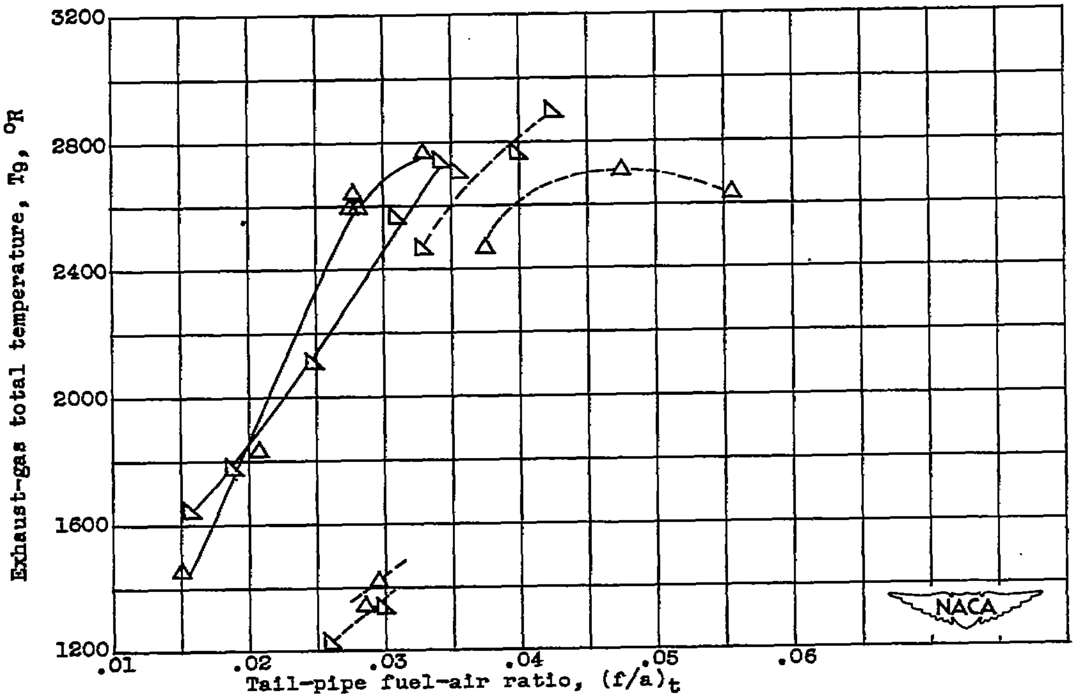

(b) Exhaust-gas total temperature.

Figure 10. - Effect of fuel-injector-bar injection on variation of exhaust-gas total temperature and combustion efficiency with tail-pipe fuel-air ratio. Flight Mach number, 0.27.

[redacted]

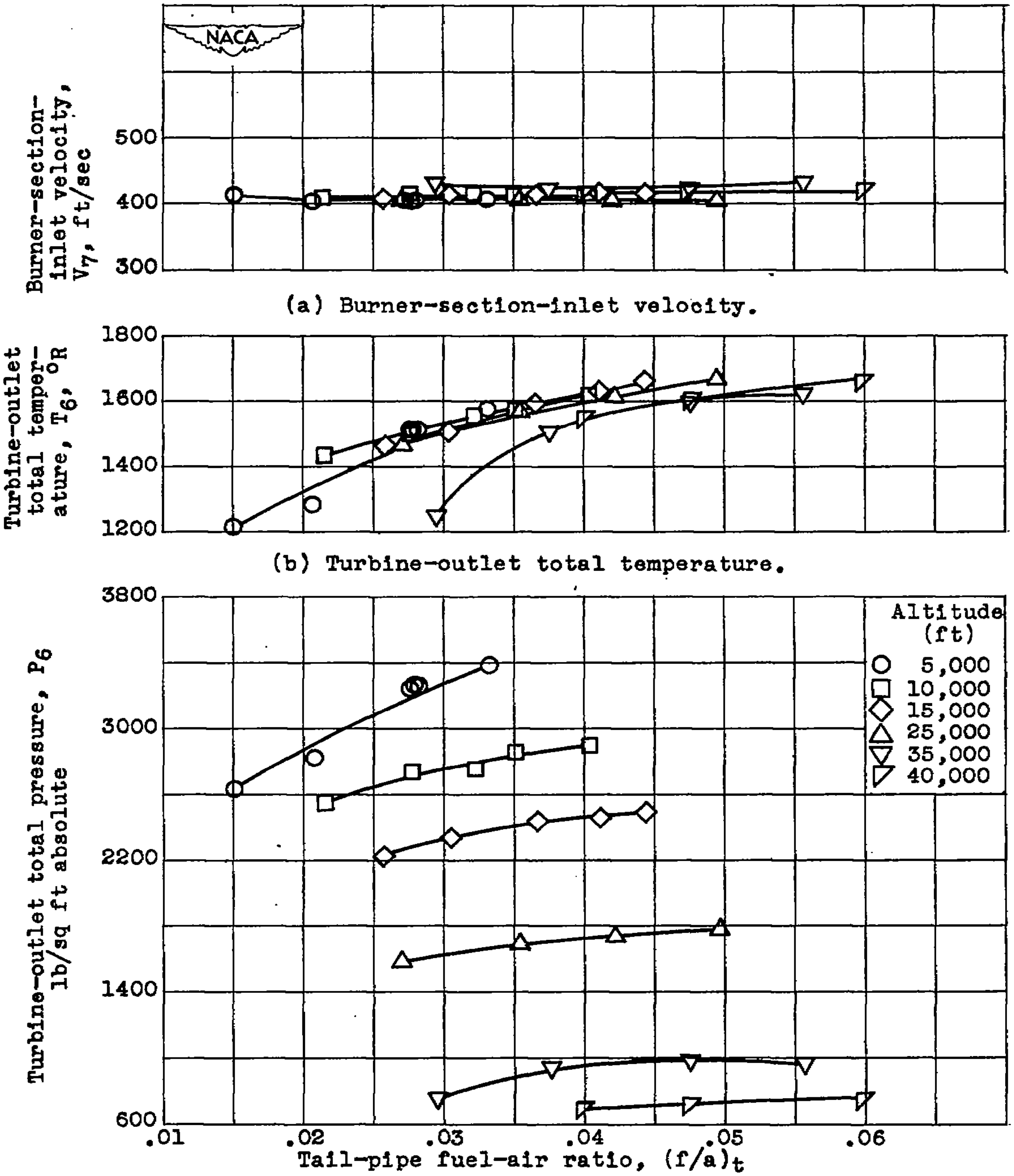

(c) Turbine-outlet total pressure.

Figure 11. - Effect of altitude on variation of burner-section-inlet velocity, turbine-outlet total temperature, and turbine-outlet total pressure with tail-pipe fuel-air ratio for configuration D. Flight Mach number, 0.27.

[redacted]

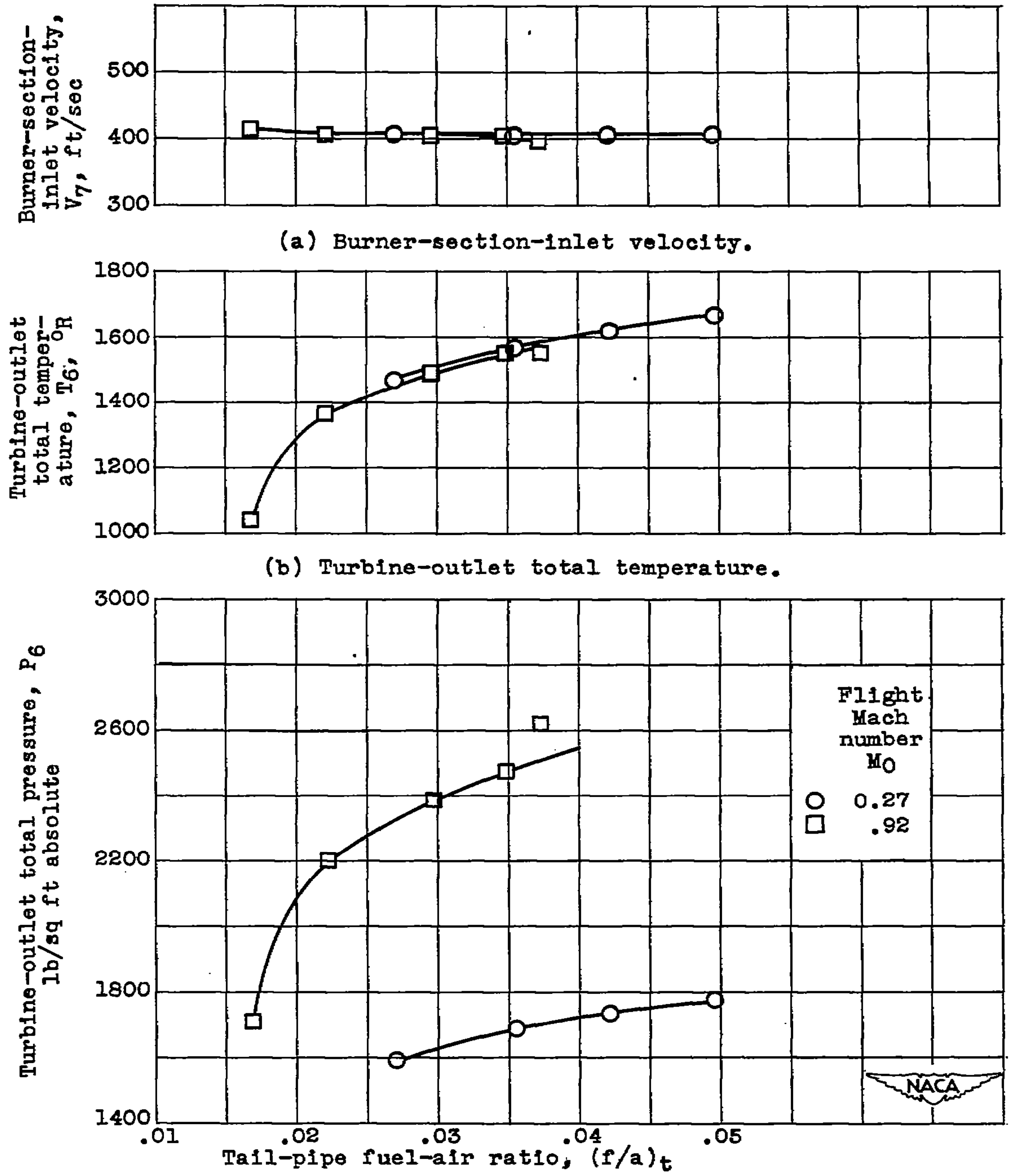

(a) Burner-section-inlet velocity.

(b) Turbine-outlet total temperature.

(c) Turbine-outlet total pressure.

Figure 12. - Effect of flight Mach number on variation of burner-section-inlet velocity, turbine-outlet total temperature, and turbine-outlet total pressure with tail-pipe fuel-air ratio for configuration D. Altitude, 25,000 feet.

[redacted]

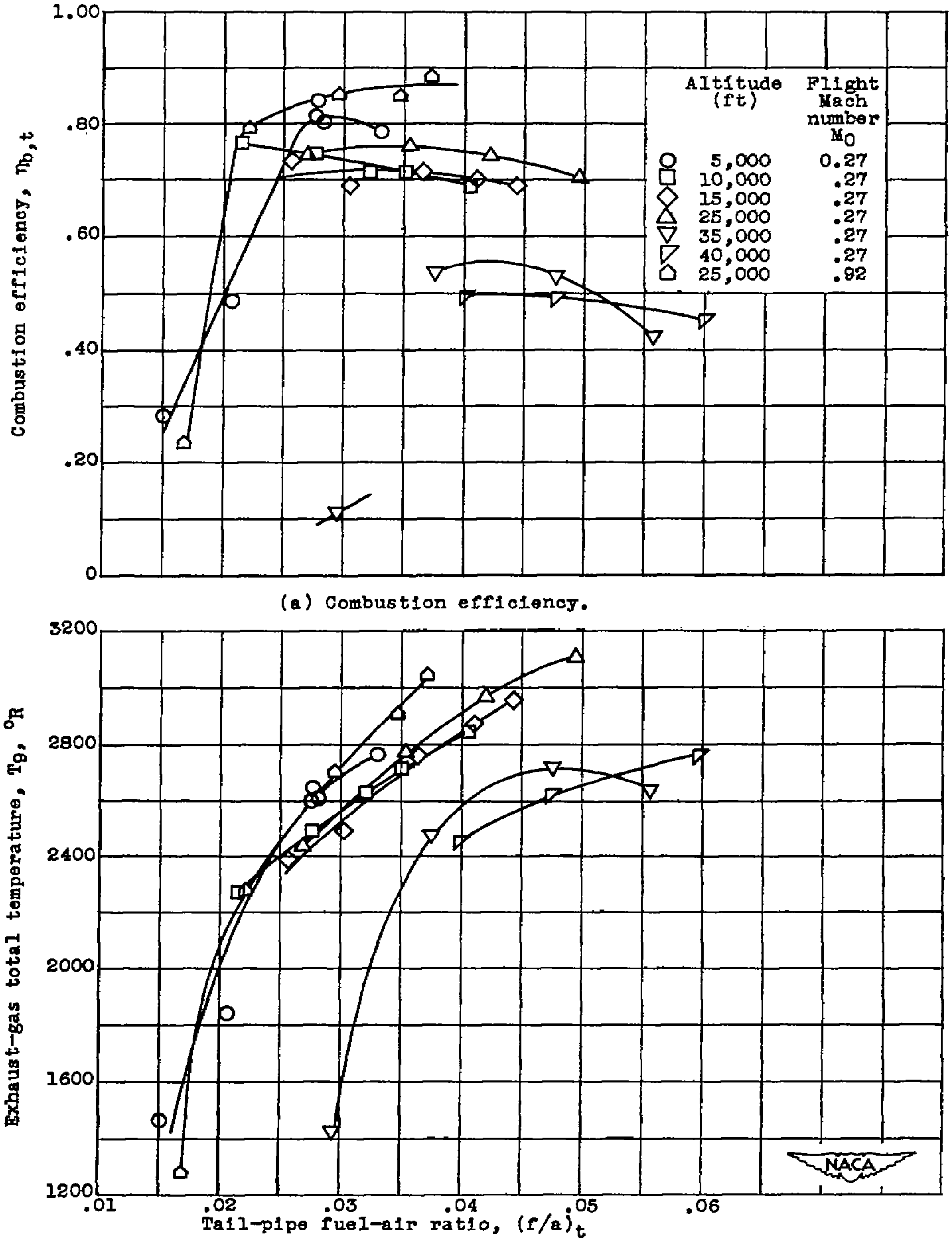

(a) Combustion efficiency.

(b) Exhaust-gas total temperature.

Figure 13. - Effect of altitude and flight Mach number on variation of exhaust-gas total temperature and combustion efficiency with tail-pipe fuel-air ratio for configuration D.

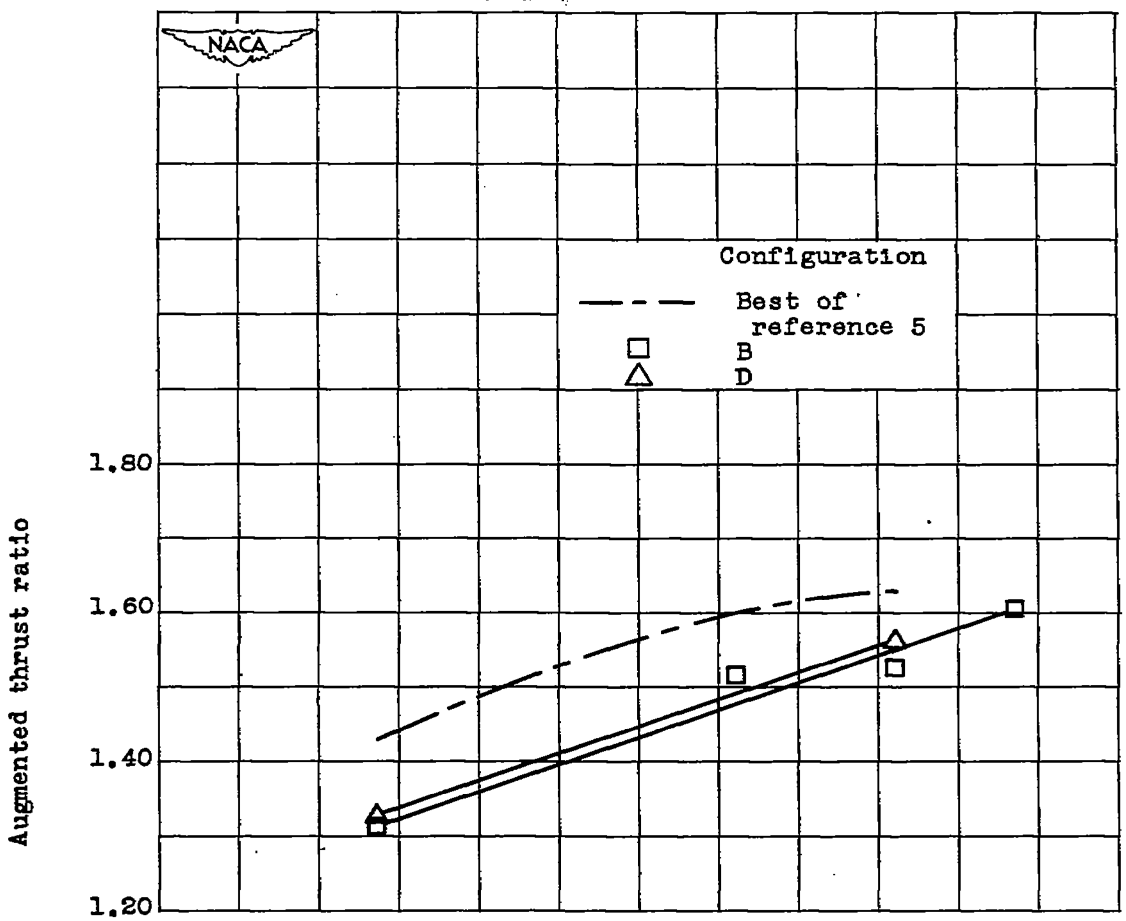

(a) Augmented thrust ratio.

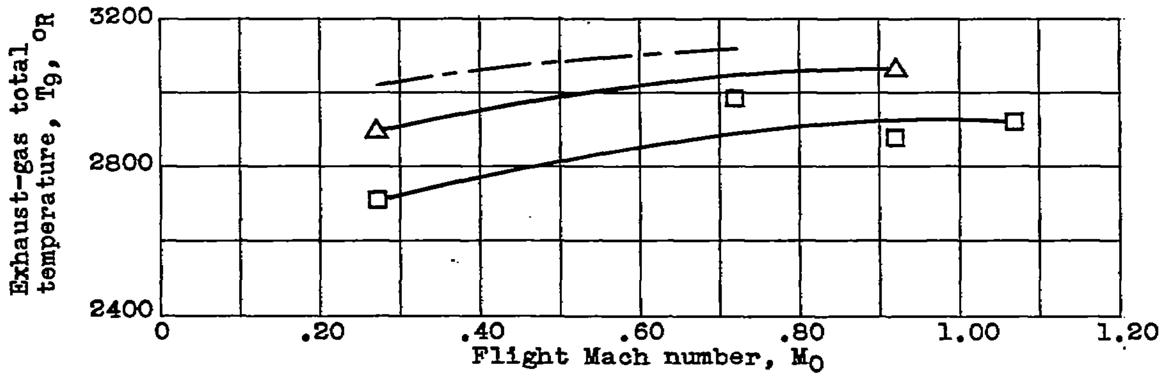

(b) Exhaust-gas total temperature.

Figure 14. - Variation of exhaust-gas total temperature and augmented thrust ratio with flight Mach number for configurations B and D and best configuration of reference 5. Turbine-outlet temperature, 1600 °R; altitude, 25,000 feet.

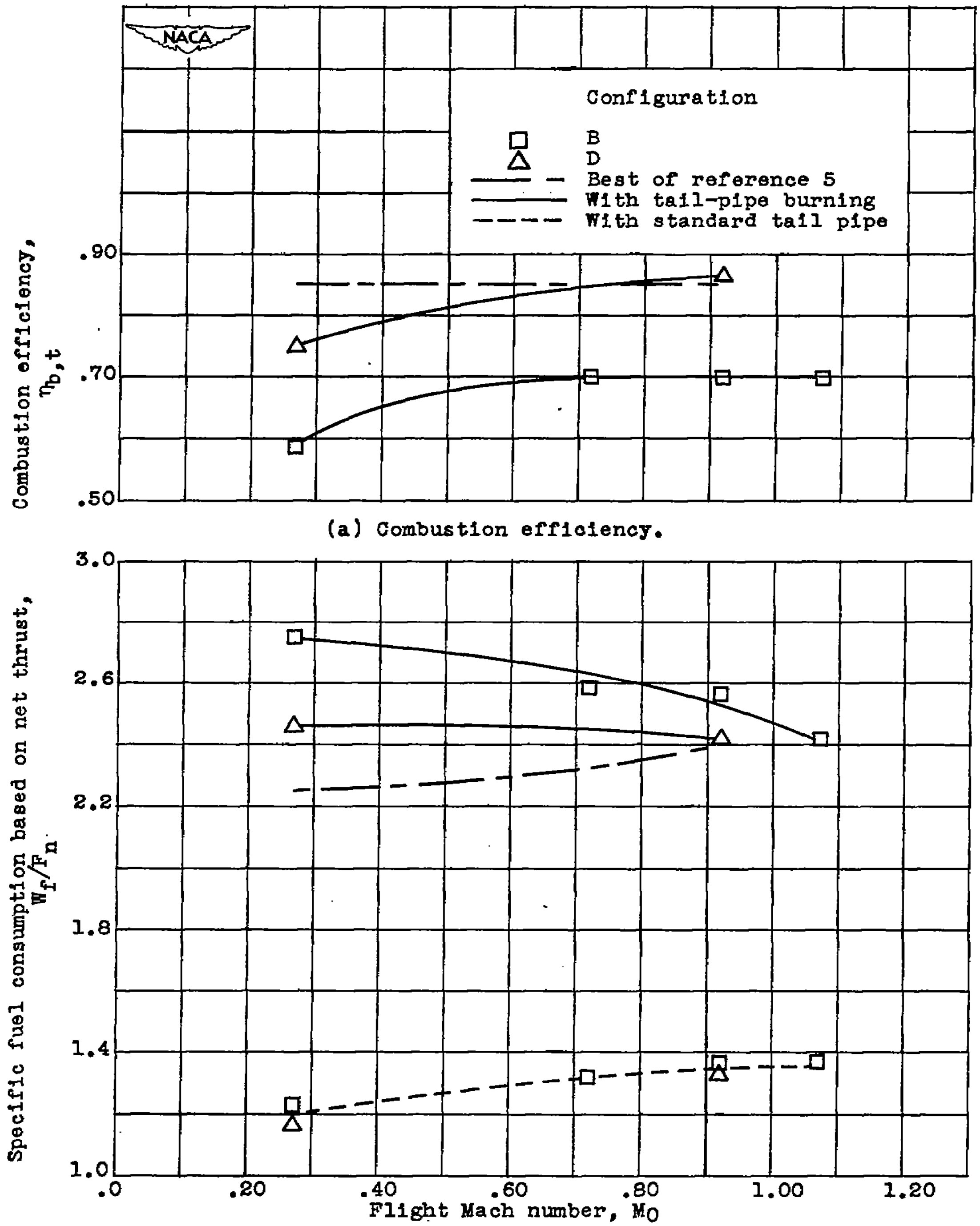

(a) Combustion efficiency.

(b) Specific fuel consumption.

Figure 15. - Variation of burner combustion efficiency and specific fuel consumption based on net thrust with flight Mach number for configurations B and D, best configuration of reference 5, and standard engine tail pipe. Turbine-outlet temperature, 1600 °R; altitude, 25,000 feet.

1245

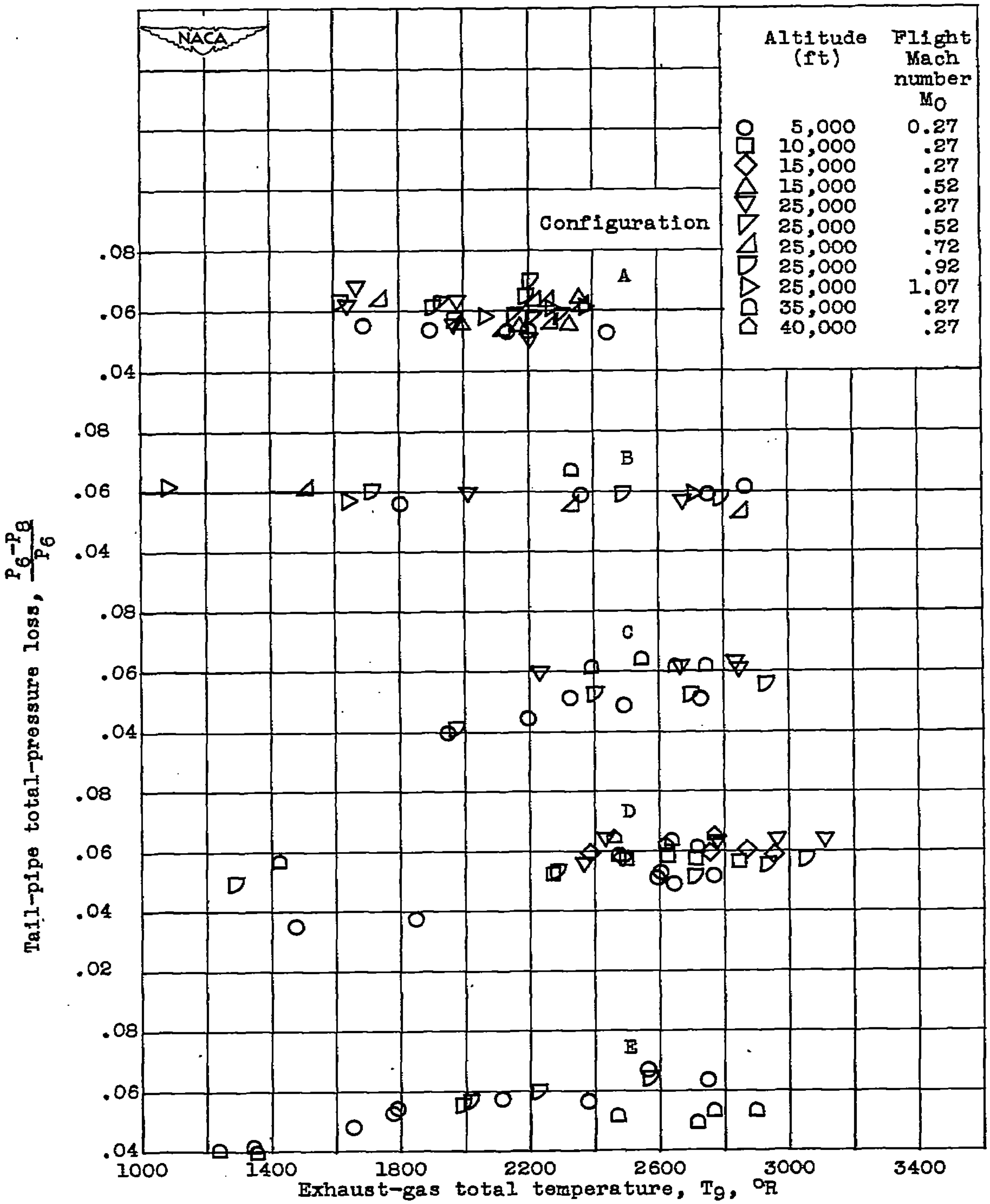

Figure 16. - Effect of altitude and flight Mach number on variation of tail-pipe-burner total-pressure loss with exhaust-gas total temperature for configurations A, B, C, D, and E.